BRAIN COMMUNICATIONS

TDP-43 cytoplasmic inclusion formation is disrupted in *C9orf72*-associated amyotrophic lateral sclerosis/frontotemporal lobar degeneration

Samuel M. Lee,[1,2] Seneshaw Asress,[1,2] Chadwick M. Hales,[1,2] Marla Gearing,[1,2,3] Juan C. Vizcarra,[4,5] Christina N. Fournier,[1,2] David A. Gutman,[4,5] Lih-Shen Chin,[2,6] Lian Li[2,6] and Jonathan D. Glass[1,2,3]

The G4C2 hexanucleotide repeat expansion mutation in the *C9orf72* gene is the most common genetic cause underlying both amyotrophic lateral sclerosis and frontotemporal dementia. Pathologically, these two neurodegenerative disorders are linked by the common presence of abnormal phosphorylated TDP-43 neuronal cytoplasmic inclusions. We compared the number and size of phosphorylated TDP-43 inclusions and their morphology in hippocampi from patients dying with sporadic versus *C9orf72*-related amyotrophic lateral sclerosis with pathologically defined frontotemporal lobar degeneration with phosphorylated TDP-43 inclusions, the pathological substrate of clinical frontotemporal dementia in patients with amyotrophic lateral sclerosis. In sporadic cases, there were numerous consolidated phosphorylated TDP-43 inclusions that were variable in size, whereas inclusions in *C9orf72* amyotrophic lateral sclerosis/frontotemporal lobar degeneration were quantitatively smaller than those in sporadic cases. Also, *C9orf72* amyotrophic lateral sclerosis/frontotemporal lobar degeneration homogenized brain contained soluble cytoplasmic TDP-43 that was largely absent in sporadic cases. To better understand these pathological differences, we modelled TDP-43 inclusion formation in fibroblasts derived from sporadic or *C9orf72*-related amyotrophic lateral sclerosis/frontotemporal dementia patients. We found that both sporadic and *C9orf72* amyotrophic lateral sclerosis/frontotemporal dementia patient fibroblasts showed impairment in TDP-43 degradation by the proteasome, which may explain increased TDP-43 protein levels found in both sporadic and *C9orf72* amyotrophic lateral sclerosis/frontotemporal lobar degeneration frontal cortex and hippocampus. Fibroblasts derived from sporadic patients, but not *C9orf72* patients, demonstrated the ability to sequester cytoplasmic TDP-43 into aggresomes via microtubule-dependent mechanisms. TDP-43 aggresomes *in vitro* and TDP-43 neuronal inclusions *in vivo* were both tightly localized with autophagy markers and, therefore, were likely to function similarly as sites for autophagic degradation. The inability for *C9orf72* fibroblasts to form TDP-43 aggresomes, together with the observations that TDP-43 protein was soluble in the cytoplasm and formed smaller inclusions in the *C9orf72* brain compared with sporadic disease, suggests a loss of protein quality control response to sequester and degrade TDP-43 in *C9orf72*-related diseases.

1 Department of Neurology, Emory University School of Medicine, Atlanta, GA 30322, USA
2 Center for Neurodegenerative Disease, Emory University School of Medicine, Atlanta, GA 30322, USA
3 Department of Pathology & Laboratory Medicine, Emory University School of Medicine, Atlanta, GA 30322, USA
4 Department of Biomedical Engineering, Emory University School of Medicine, Atlanta, GA 30322, USA
5 Department of Biomedical Engineering, Georgia Institute of Technology, Atlanta, GA 30332, USA
6 Department of Pharmacology, Emory University School of Medicine, Atlanta, GA 30322, USA

Received July 2, 2019. Revised August 10, 2019. Accepted August 19, 2019. Advance Access publication September 11, 2019

Correspondence to: Lian Li, Ph.D
Department of Pharmacology
Emory University School of Medicine
1510 Clifton Road, Atlanta, GA 30322, USA
E-mail: lli5@emory.edu

Correspondence may also be addressed to: Jonathan D. Glass, M.D.
Department of Neurology
Emory University School of Medicine
1365 Clifton Road, Atlanta, GA 30322, USA
E-mail: jglas03@emory.edu

Keywords: TDP-43; inclusion formation; aggresome; frontotemporal dementia; amyotrophic lateral sclerosis

Abbreviations: : ALS = amyotrophic lateral sclerosis; C9 = C9orf72; FTD = frontotemporal dementia; FTLD = frontotemporal lobar degeneration; HRE = hexanucleotide repeat expansion; pTDP-43 = phosphorylated TAR DNA-binding protein 43; TDP-43 = TAR DNA-binding protein 43; UPS = ubiquitin-proteasome system

Graphical Abstract

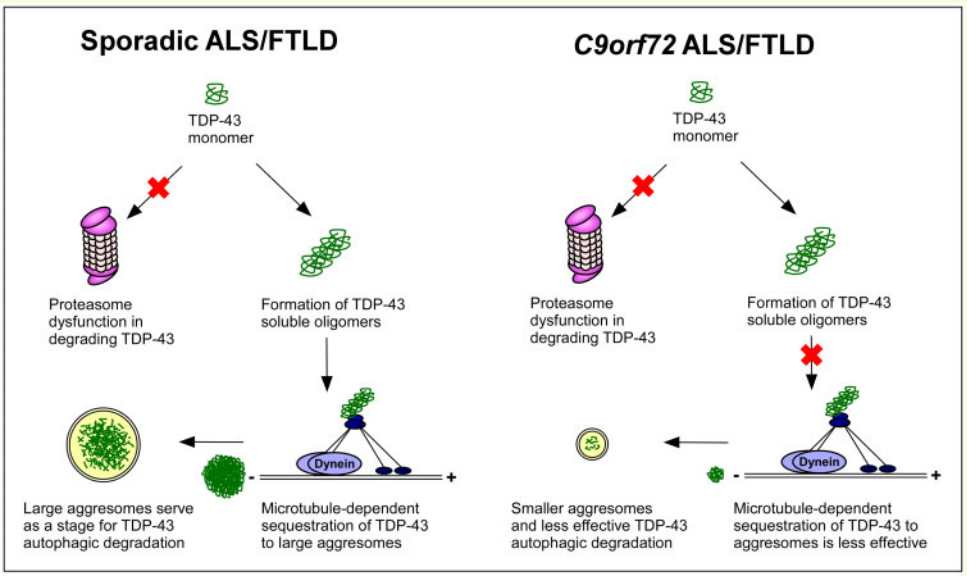

Introduction

TDP-43 proteinopathies such as amyotrophic lateral sclerosis (ALS) and frontotemporal lobar degeneration (FTLD) are progressive neurodegenerative diseases pathologically characterized by the presence of TAR DNA-binding protein 43 (TDP-43) neuronal cytoplasmic inclusions (Seelaar *et al.*, 2007; Blokhuis *et al.*, 2013). In addition to shared TDP-43 pathology, ALS and FTLD present as a clinical spectrum (Hinz and Geschwind, 2017). Approximately 15% of patients with clinical manifestation of FTLD, i.e. frontotemporal dementia (FTD), is diagnosed with ALS, and up to 30% of ALS patients meet the diagnostic criteria for FTD (Hinz and Geschwind, 2017). These shared pathologies and overlapping clinical presentations, together with the discovery of the G4C2 hexanucleotide repeat expansion (HRE) mutation in the *C9orf72* gene as the most common genetic cause of ALS and/or FTLD (ALS/FTLD; Renton *et al.*, 2011; Rademakers, 2012), suggest common pathogenic mechanisms for ALS and FTLD. Patients with *C9orf72*-related ALS/FTD are clinically indistinguishable from those with sporadic ALS/FTD (Sha *et al.*, 2012). Pathologically, *C9orf72*-associated disease is characterized by the pathognomonic finding of cerebellar neuronal inclusions that are positive by immunohistochemistry for p62 (sequestosome-1), but negative for phosphorylated TDP-43 (pTDP-43; Pikkarainen *et al.*, 2010; Al-Sarraj *et al.*, 2011; Bigio *et al.*, 2013).

TDP-43 is essential for regulating transcriptional events (Sephton *et al.*, 2012) and its expression level in neurons is tightly regulated (Polymenidou *et al.*, 2011). Previous studies reported that expression of exogenous human TDP-43 protein in transgenic mice causes neurodegeneration (Wils *et al.*, 2010; Igaz *et al.*, 2011), suggesting that excess TDP-43 could be toxic to the central nervous system. TDP-43 is prone to spontaneous aggregation into oligomers that are cytotoxic (Johnson *et al.*, 2009; Takalo *et al.*, 2013), which supports a role for the

overabundance of TDP-43 to cause neuronal injury. However, it remains unknown whether an increase of TDP-43 protein level is linked to ALS and FTLD pathogenesis because the protein level of TDP-43 in the brains of ALS and FTLD patients has not been established. Although dysfunction in protein quality control systems that target excess proteins for degradation, such as the ubiquitin-proteasome system (UPS; Ciechanover, 1994) and the autophagy pathway (Klionsky *et al.*, 2012), have been proposed for ALS and FTLD pathogenesis (Shahheydari *et al.*, 2017), it is unclear whether these pathways are affected in sporadic and *C9orf72*-associated ALS and FTLD patients.

The mechanisms responsible for TDP-43 pathology in sporadic and *C9orf72*-associated ALS and FTLD remain largely unknown. Differences in p62 inclusions between sporadic and *C9orf72*-associated ALS and FTLD in the cerebellum prompted us to determine whether TDP-43 inclusion body formation is different between sporadic and *C9orf72*-associated ALS and FTLD, which may provide valuable insights into the pathogenesis of these diseases. Studies of TDP-43 inclusions in the FTLD brain is difficult because the concomitant diagnosis of ALS can affect FTLD pathology (Mackenzie *et al.*, 2006; Cairns *et al.*, 2007; Mackenzie *et al.*, 2011*a*). An advantage to focusing on ALS patients with FTD and FTLD is that this is a more homogeneous group of subjects to investigate the differences in TDP-43 pathology between sporadic and *C9orf72*-associated diseases. In addition to examining TDP-43 pathology *in vivo*, we also performed complimentary *in vitro* experiments using patient-derived cells to investigate differences in the underlying mechanisms of TDP-43 inclusion body formation and protein control pathways between sporadic and *C9orf72* patients. Overall, our findings demonstrate that *C9orf72* patients are characterized by unique *in vivo* and *in vitro* features in TDP-43 inclusion body formation that are distinct from sporadic cases, which may have clinical and pathophysiological implications.

Materials and methods

Patient tissue samples and generation of patient-derived fibroblasts

For pathological studies, post-mortem brain tissues were obtained from the brain bank maintained by the Emory Alzheimer Disease Research Center under proper Institutional Review Board protocols. All patients were diagnosed with ALS and were cared for at the Emory ALS Center (Umoh *et al.*, 2016). The clinical diagnosis of FTD, for selection of cases for fibroblast generation, was made based on established clinical diagnostic criteria (Rascovsky *et al.*, 2011) by an experienced neurologist (J.D.G.). The neuropathological diagnosis of FTLD with TDP-43 pathology was made by experienced neuropathologists (M.G. and J.D.G.) based on published criteria (Cairns *et al.*, 2007; Mackenzie *et al.*, 2011*b*). The presence of a *C9orf72* HRE mutation was assessed from DNA extracted from the post-mortem brains of ALS/FTLD patients using the published PCR method as described previously (DeJesus-Hernandez *et al.*, 2011; Umoh *et al.*, 2016). Clinical and pathological information from all individual cases, including disease status, age, sex and post-mortem interval are provided in Supplementary Table 1 and summarized in Supplementary Table 2. All patients with ALS/FTLD had a clinical diagnosis of ALS with behavioural variant FTD.

For the generation of fibroblast lines, patients diagnosed clinically as ALS/FTD or ALS underwent skin biopsy after informed consent was obtained from the patient and the patient's legal power of attorney. Samples were de-identified and processed as described previously to obtain fibroblasts (Konrad *et al.*, 2017). Fibroblasts were cultured in Dulbecco's modified Eagle medium supplemented with 10% foetal bovine serum. Cultured fibroblasts were studied at passages ranging between 7 and 15. Experiments with patient-derived fibroblasts were approved by the Institutional Review Board at Emory University (IRB00064365).

Immunohistochemistry of brain tissue

Paraffin-embedded sections from frontal cortex, hippocampus, occipital cortex and cerebellum (8 µm thickness) were de-paraffinized by incubation at 60°C for 30 min and rehydrated by immersion in graded ethanol solutions. Antigen retrieval was by microwaving in 10 mM citrate buffer (pH 6.0) for 5 min followed by allowing slides to cool to room temperature for 30 min. Endogenous peroxidase activity was eliminated by incubating slides with hydrogen peroxide block solution (Fisher) for 10 min at room temperature followed by rinsing in phosphate buffered saline. Non-specific binding was reduced by blocking in ultraVision Block (Fisher) for 5 min at room temperature. Sections were then incubated overnight with primary antibodies (refer to Supplementary Table 3 for a full list of antibodies used in this study) diluted in 1% BSA in phosphate buffered saline for 30 min in room temperature or incubated without primary antibody as a negative control. Sections were rinsed in phosphate buffered saline and incubated in labelled ultraVision LP detection system horseradish peroxidase-polymer secondary antibody (Fisher) for 15 min at room temperature. Slides were imaged for analysis using an Aperio Digital Pathology Slide Scanner (Leica Biosystems). For immunofluorescence, slides were processed as described above except that fluorescent secondary antibodies (Jackson ImmunoResearch Laboratories) were used instead of

biotinylated antibodies. Tissue sections were analysed using immunofluorescence confocal microscopy as described previously (Lee *et al.*, 2011, 2012).

Quantification of inclusions in the hippocampus

Hippocampal sections were chosen for quantification analyses because this brain region was routinely examined in previous reports of *C9orf72*-associated FTLD cases and is known to have abundant TDP-43 inclusions in FTLD cases (Al-Sarraj *et al.*, 2011; Bigio *et al.*, 2013). For the quantification of TDP-43 and p62 neuronal cytoplasmic inclusions, sections stained with an antibody against pTDP-43 (Seilhean *et al.*, 2009; Brettschneider *et al.*, 2014) or p62 were analysed. The dentate gyrus in each image was manually annotated as the region of interest using custom JavaScript web-based applications. Images then underwent colour normalization using the Reinhard method (Reinhard *et al.*, 2001) and colour deconvolution into two separate channels to discriminate the neuronal nuclei stained with haematoxylin from pTDP-43 or p62 inclusions visualized by 3,3′-diaminobenzidine chromogen. For each channel, Laplacian-of-Gaussian filtering as applied by the HistomicsTK Python toolkit (GitHub, https://github.com/DigitalSlideArchive/HistomicsTK) was used, and the Al-Kofahi method (Al-Kofahi *et al.*, 2010) was used to detect individual nuclei and inclusions. To prevent background staining from being counted as an inclusion, we calculated the Euclidean distance from the middle point of each pTDP-43 or p62 marking to the middle point of every nucleus and excluded any immunostaining that was not near any nucleus as determined by a pre-defined threshold. Using these methods, the inclusion sizes, the total number of hippocampal inclusions, the total number of hippocampal neuronal nuclei, the number of inclusions per non-overlapping low-power field, the number of neuronal nuclei per non-overlapping low-power field and the area of each inclusion were measured. The median inclusion sizes and the percentages of neurons with pTDP-43 inclusions and/or p62 inclusions were calculated for the entire hippocampus from each case. In addition, the percentages of hippocampal neurons with pTDP-43 inclusions from at least 20 low-power fields were determined and averaged for each case. Statistical analyses of the inclusion sizes and the percentages of neurons with inclusions were performed using individual cases as the experimental unit.

For quantification of double immunofluorescence staining, hippocampal sections stained with antibodies against p62 and the C-terminal of TDP-43 were subjected to confocal microscopic analyses. The C-terminal TDP-43 antibody, in contrast to the pTDP-43 antibody, reacts with all species of TDP-43 protein. Low-power field images were examined in a blinded manner and scored for the number of TDP-43-positive/p62-positive (defined as p62-positive inclusion that co-localized with TDP-43) and TDP-43-negative/p62-positive (defined as p62-positive inclusion that did not co-localize with TDP-43) inclusions. The total number of hippocampal cells in each field was determined by 4′,6-diamidino-2-phenylindole (DAPI) staining. The percentages of hippocampal cells with each type of inclusion were determined and averaged from at least 10 low-power fields per case. Statistical analyses of the percentages of hippocampal cells with inclusions were performed using individual cases as the experimental unit.

Fractionation of human frontal cortex tissue

Frozen frontal cortex tissue (~0.1 mg) was randomly selected from three to five patients per group by our co-author (S.A.) who was blinded to group (three control patients, three C9orf72 ALS/FTLD and five sporadic ALS/FTLD cases total). The tissue was thawed in 1 ml of ice-cold homogenization buffer (10 mM HEPES/KOH, pH 7.4, 1 mM EDTA) containing 250 mM sucrose, and homogenates were centrifuged at 10 000 g for 10 min to pellet the non-soluble nuclei/unbroken cells/inclusion bodies fraction and to obtain the supernatant as the soluble cytosol fraction as previously described (Shaiken and Opekun, 2014). Equal volumes of the total, nuclear/unbroken cells/inclusion bodies and cytosol fractions were analysed by sodium dodecyl sulfate polyacrylamide gel electrophoresis (SDS-PAGE) and by sequential immunoblotting for TDP-43, the nuclear marker NeuN (Aber *et al.*, 2003; Misztal *et al.*, 2017), the cytosolic marker glyceraldehyde 3-phosphate dehydrogenase (GADPH) and actin. Soluble cytoplasmic TDP-43 protein levels from non-over-exposed images obtained using the Bio-Rad ChemiDoc MP imaging system were quantified (Giles *et al.*, 2008; Lee *et al.*, 2011) using NIH ImageJ and were normalized to total TDP-43 protein level. To further control for protein quantities in each fraction, soluble cytoplasmic and total TDP-43 protein levels were normalized to the cytoplasmic and total GADPH protein levels, respectively, followed by normalization of soluble TDP-43 protein level to total TDP-43 protein level.

Quantification of TDP-43 level in brain tissues

Frozen brain tissue from the frontal cortex, hippocampus, occipital cortex and cerebellum were homogenized with a Teflon-glass homogenizer in 10 volumes of 1% SDS, followed by a combination of boiling and sonification. An equal amount of total proteins from each lysate was subjected to immunoblot analyses. TDP-43 protein levels from non-over-exposed images obtained using the Bio-Rad ChemiDoc MP imaging system were quantified as described (Giles *et al.*, 2008; Lee *et al.*, 2011) using NIH ImageJ and were normalized to actin protein level. Actin was chosen as an appropriate loading control since its protein level is not significantly altered between control,

C9orf72 ALS/FTLD, sporadic ALS/FTLD and sporadic ALS tissues from various brain regions when normalized to the corresponding total protein as determined by Ponceau S staining (data not shown).

Treatment of fibroblasts with proteasome and autophagy inhibitors

Fibroblasts from two control patients, three *C9orf72* patients (one with clinical ALS/FTD and two with clinical ALS) and three sporadic patients (one with clinical ALS/FTD and two with clinical ALS) were incubated for 24 h at 37°C with proteasome inhibitor MG132 (20 μM, Sigma), autophagy inhibitor bafilomycin A1 (50 nM, Sigma), or vehicle (0.1% DMSO) as described previously (Giles *et al.*, 2008; Lee *et al.*, 2011). For immunoblot analysis, fibroblasts were lysed with 1% SDS, and an equal amount of total protein from each lysate was analysed by SDS-PAGE. The protein levels of TDP-43 were quantified using NIH ImageJ (Giles *et al.*, 2008; Lee *et al.*, 2011) and then normalized to the corresponding actin levels. Quantification of LC3-II/LC3-I ratio was performed as described previously (Klionsky *et al.*, 2012).

Immunocytochemistry and quantification of co-localization and signal intensity

Fibroblasts were fixed in 4% paraformaldehyde and processed for immunofluorescence confocal microscopy as described previously (Olzmann *et al.*, 2007; Lee *et al.*, 2012). The percentage of co-localization for each cell was determined by the percentage of the immunostaining by the first primary antibody [anti-pTDP-43 (Seilhean *et al.*, 2009; Sabatelli *et al.*, 2015), anti-TDP-43 or anti-p62] that was co-localized with the immunostaining by the second primary antibody (anti-p62 or anti-TDP-43) or with DAPI staining. Co-localization was quantified on unprocessed images of cells double-labelled for TDP-43, p62 and/or DAPI as previously described (Webber *et al.*, 2008; Lee *et al.*, 2011). Single cells were selected by manually tracing the cell outlines. The background was subtracted and the percentage of the first primary antibody overlapping with the second primary antibody or DAPI staining was determined for each cell (Webber *et al.*, 2008; Lee *et al.*, 2011). The signal intensities of pTDP-43 and p62 immunostaining were quantified on unprocessed images of cells stained with either pTDP-43 or p62 as previously described (Lee *et al.*, 2012). Single cells were selected and with background subtracted as above, and the signal intensity for either pTDP-43 or p62 was measured with NIS Elements (Nikon) and normalized to DAPI signal intensity level for each cell (Kreiling *et al.*, 2011; Serebryannyy *et al.*, 2016). For statistical analyses of signal intensity and co-localization, results from at least 30 randomly selected cells were averaged per patient, and analyses were performed using individual cases as the experimental unit. Fibroblasts from two control patients, three *C9orf72* patients (one with clinical ALS/FTD and two with clinical ALS) and three sporadic disease patients (one with clinical ALS/FTD and two with clinical ALS) were analysed.

Statistical analysis

Data were subjected to statistical analyses by Student's *t*-tests, one-way ANOVA or two-way ANOVA using the SigmaPlot software (Systat Software, Inc.) Results were expressed as mean ± standard error of the mean (SEM). A P-value of <0.05 was considered statistically significant. The experimental units, the specific statistical tests, the test statistics, degrees of freedom as subscripts to the test statistic and the exact P-values were reported in Supplementary Table 4.

Data availability

The data supporting the findings of this study are available from the corresponding authors upon reasonable request.

Results

Sporadic ALS/FTLD brain has more frequent and larger pTDP-43 inclusions compared with *C9orf72* brain

Using a phospho-TDP-43-specific antibody, we performed immunohistochemistry on *C9orf72* ALS/FTLD brain and confirmed the pathognomonic findings of p62-positive inclusions in the absence of pTDP-43 inclusions in the cerebellum (Supplementary Fig. 1). In contrast, sporadic ALS/FTLD brains showed complete absence of pTDP-43 and p62 inclusions in the cerebellum (Supplementary Fig. 1). We further compared sporadic and *C9orf72* disease pathology in the hippocampus with quantification analyses and found that sporadic ALS/FTLD brain contains numerous round and circumferential pTDP-43 inclusions throughout the hippocampal dentate gyrus as previously reported (Tan *et al.*, 2017), whereas hippocampal pTDP-43 inclusions were notably less obvious in *C9orf72* patients (Fig. 1A). Quantitative analyses showed that sporadic ALS/FTLD cases demonstrated a trend to having more overall pTDP-43 inclusions in the hippocampus compared with *C9orf72* patients, though this did not meet statistical significance (Supplementary Fig. 2A). However, pTDP-43 inclusions were more frequently seen in sporadic ALS/FTLD when quantifying the density of pTDP-43 inclusions under low-power fields for each case and analysed using each case as the experimental unit

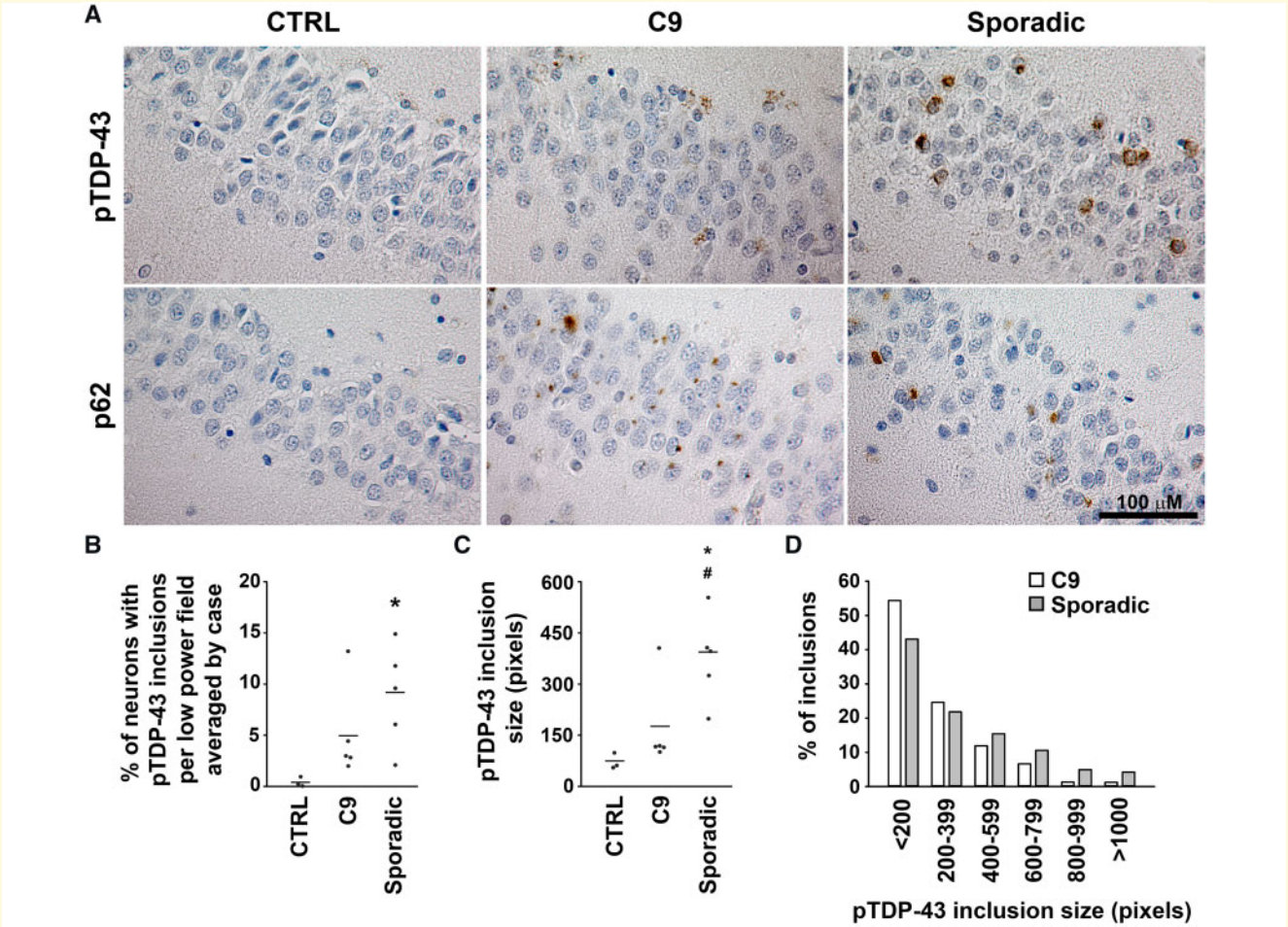

Figure 1 pTDP-43 inclusions are more frequent and larger in sporadic compared with *C9orf72* ALS/FTLD hippocampus. (**A**) Paraffin-embedded sections from the dentate gyrus of the hippocampus were subjected to immunohistochemistry with anti-pTDP-43 antibody or anti-p62 antibody and counterstained with haematoxylin. (**B**) The percentages of neurons with pTDP-43 inclusions in low-power fields were determined and averaged for each case and analysed using each case as the experimental unit as described in the Materials and Methods section. (**C**) The sizes of pTDP-43 inclusions were determined for each case, and the median inclusion sizes for these cases were compared among control, *C9orf72* and sporadic ALS/FTLD hippocampi as described in the Materials and Methods section. The mean for each experimental group was represented by a horizontal line. $^{*}P < 0.05$ compared with control and $^{\#}P < 0.05$ compared with *C9orf72* ALS/FTLD based on one-way ANOVA and post-hoc Tukey's test. (**D**) Histogram showing the percentages of pTDP-43 inclusions of different sizes in *C9orf72* and sporadic ALS/FTLD hippocampi. C9, *C9orf72*; CTRL, control; pTDP-43, phosphorylated TDP-43.

(Fig. 1B). In contrast to pTDP-43 inclusions, p62 inclusions were significantly more numerous in the hippocampal dentate gyrus of *C9orf72* patients compared with sporadic patients (Fig. 1A, Supplementary Fig. 2B). Another notable finding was that pTDP-43 inclusions in the hippocampus of *C9orf72* patients were quantitatively smaller than those seen in sporadic cases (Fig. 1A, C and D). Both round and circumferential pTDP-43 inclusions were also found in the frontal cortex of sporadic ALS/FTLD cases but were less obvious in *C9orf72* ALS/FTLD frontal cortex (Supplementary Fig. 3). These findings were not influenced by TDP-43 inclusion subtypes (Mackenzie *et al.*, 2006; Cairns *et al.*, 2007; Mackenzie *et al.*, 2011*a*). The results illustrated in Fig. 1B and C were unchanged when only cases with TDP-43 type B inclusions were present in the quantification analyses (data not shown). Compared with the dentate gyrus and frontal cortex, pTDP-43 inclusions were rarely found in the occipital cortex and absent in the cerebellum in sporadic and *C9orf72* ALS/FTLD (Supplementary Figs. 1 and 3).

Cytosolic TDP-43 is soluble in *C9orf72* ALS/FTLD brain but forms inclusions in sporadic cases

To further define TDP-43 pathology in sporadic and *C9orf72* ALS/FTLD brains, we chose a well-characterized antibody against the C-terminal of TDP-43 that detects both phosphorylated and non-phosphorylated forms of full-length TDP-43 and its C-terminal fragments (Wils *et al.*, 2010). We found that the frontal cortex and hippocampus (Fig. 2A) of sporadic ALS/

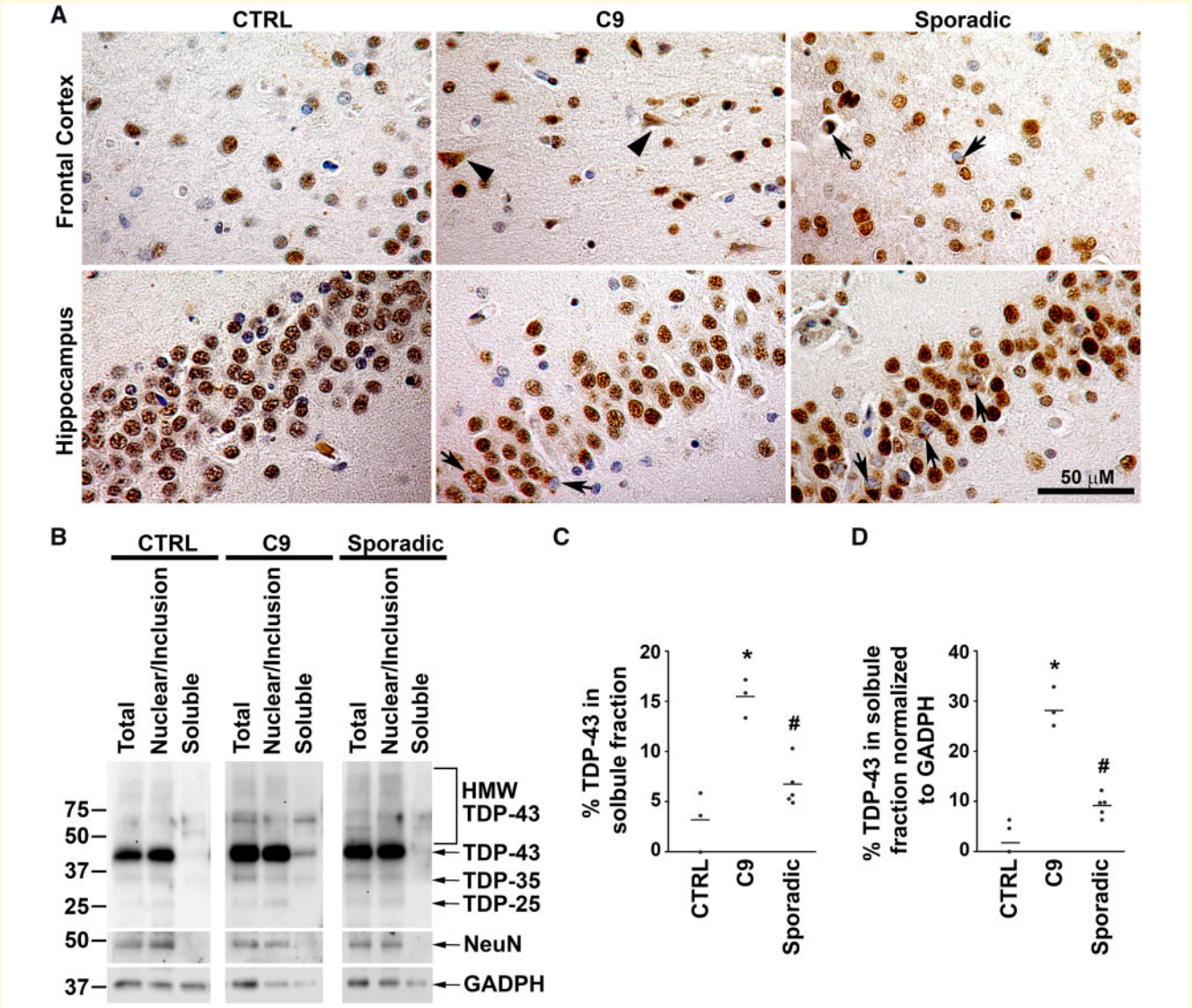

Figure 2 TDP-43 is soluble in the cytoplasm of *C9orf72* ALS/FTLD brain but not sporadic ALS/FTLD brain. (**A**) Paraffin-embedded sections from the frontal cortex and dentate gyrus of the hippocampus were subjected to immunohistochemistry with anti-C-terminal TDP-43 antibody and counterstained with haematoxylin. Black arrows indicate examples of TDP-43 neuronal cytoplasmic inclusions. Black arrow heads indicate examples of neurons with diffuse cytosolic TDP-43 staining. (**B**) Total lysates from the frontal cortex were separated into nuclear/inclusion fraction and soluble fraction. Aliquots representing an equal percentage of each fraction were subjected to immunoblot analysis with antibodies against C-terminal of TDP-43, GADPH and NeuN. The proportion of TDP-43 protein in the soluble fraction was higher in *C9orf72* tissue (**C**) and also after normalization to GADPH (**D**). The mean for each experimental group was represented by a horizontal line. $^{*}P < 0.05$ compared with control and $^{\#}P < 0.05$ compared with *C9orf72* ALS/FTLD based on one-way ANOVA and post-hoc Tukey's test. C9, *C9orf72*; CTRL, control; GADPH, glyceraldehyde 3-phosphate dehydrogenase; HMW TDP-43, higher molecular weight species identified by the C-terminal anti-TDP-43 antibody.

FTLD brain contained abundant TDP-43 cytoplasmic neuronal inclusions. These inclusions had the same morphologies as those detected using the anti-pTDP-43 antibody. In contrast to sporadic ALS/FTLD, the C-terminal TDP-43 antibody detected fewer neurons with TDP-43 cytoplasmic inclusions in *C9orf72* ALS/FTLD brains (Fig. 2A). In addition to consolidated TDP-43 inclusions, the C-terminal TDP-43 antibody identified a subpopulation of neurons in *C9orf72* ALS/FTLD with diffuse cytoplasmic staining in the frontal cortex (Fig. 2A, Supplementary Table 1). This diffuse immunostaining by the C-terminal TDP-43 antibody was distinct from the inclusion morphology identified by pTDP-43 antibody in *C9orf72* ALS/FTLD brains (Fig. 1A), and was not always associated with complete loss of nuclear TDP-43 expression (i.e. nuclear clearing) as typically reported with TDP-43 cytoplasmic inclusions (Neumann *et al.*, 2006). In contrast, neurons with

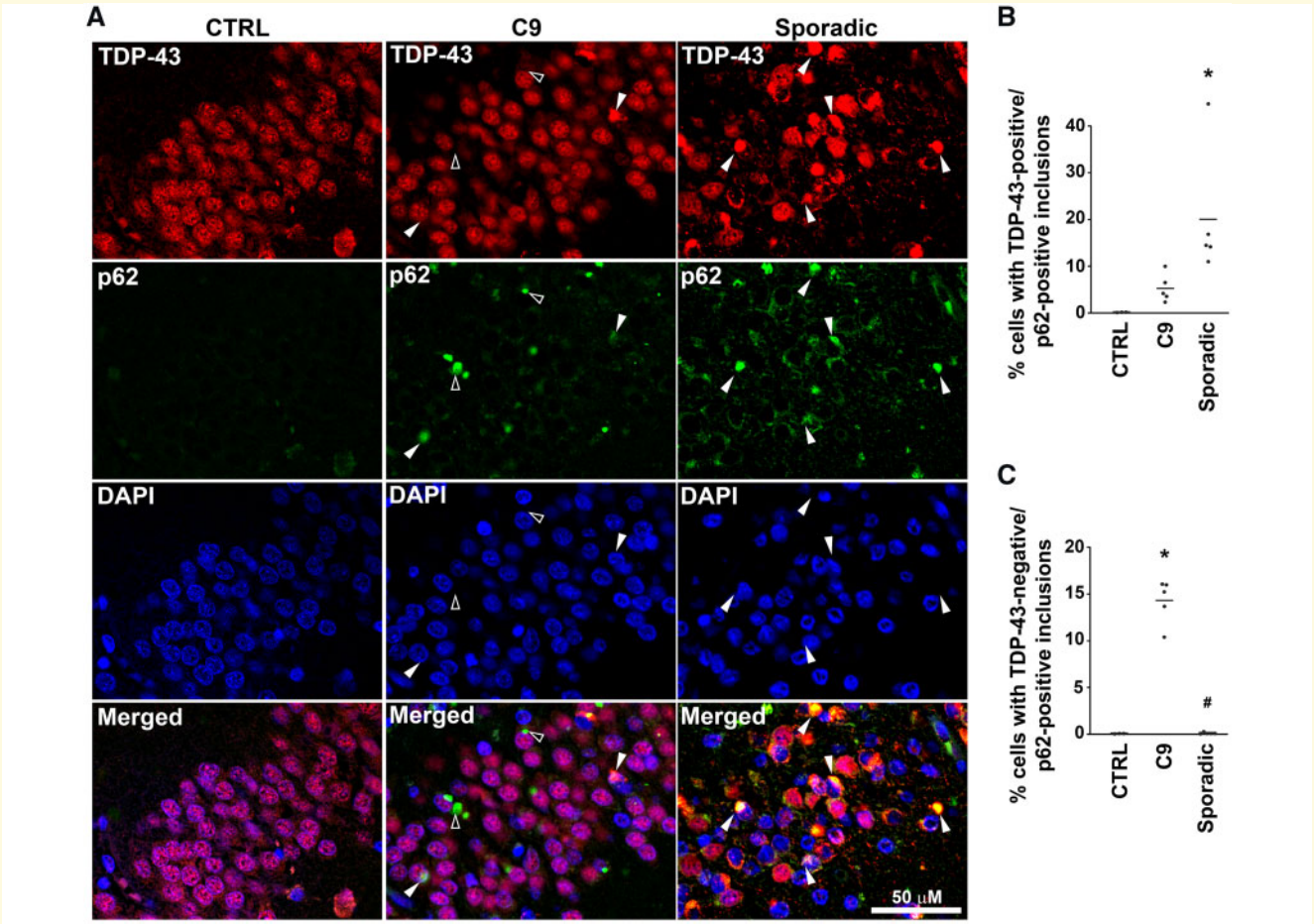

Figure 3 *C9orf72* ALS/FTLD hippocampus showed more TDP-43-negative/p62-positive inclusions compared with sporadic cases. (**A**) Paraffin-embedded sections from the hippocampus were subjected to double immunofluorescence histochemistry with anti-C-terminal TDP-43 (red) and p62 (green) antibodies. White arrow heads indicate examples of neurons with TDP-43-positive/p62-positive inclusions. Open arrow heads indicate examples of neurons with TDP-43-negative/p62-positive inclusions. Nuclei were visualized by DAPI stain (blue). The percentages of cells with TDP-43-positive/p62-positive (**B**) and TDP-43-negative/p62-positive (**C**) inclusions were determined as described in the Materials and Methods section and analysed using each case as the experimental unit. The mean for each experimental group was represented by a horizontal line. $^{*}P < 0.05$ compared with control and $^{\#}P < 0.05$ compared with *C9orf72* ALS/FTLD based on one-way ANOVA and post-hoc Tukey's test. C9, *C9orf72*; CTRL, control; sporadic, sporadic ALS/FTLD.

TDP-43 cytoplasmic inclusions did show nuclear clearing (Fig. 2A).

To determine whether the diffuse cytoplasmic TDP-43 staining seen in *C9orf72* brain represents mis-localization of soluble, cytoplasmic TDP-43, we performed subcellular fractionation of frontal cortex from *C9orf72* and sporadic ALS/FTLD patients. We isolated a fraction consisting of soluble cytosolic proteins and another fraction containing the nucleus, unbroken cells and inclusion bodies (Fig. 2B, Supplementary Fig. 4). Our results showed that *C9orf72* frontal cortex contained a soluble cytosolic fraction of TDP-43 that was absent in control and minimally present in sporadic ALS/FTLD frontal cortices (Fig. 2B–D), suggesting that the diffuse cytosolic staining seen by immunohistochemistry in *C9orf72* likely represents soluble cytoplasmic TDP-43.

C9orf72 ALS/FTLD is characterized by TDP-43 negative/p62-positive inclusions

We addressed the occurrence of co-aggregation of TDP-43 and p62 using double fluorescence immunohistochemistry. In sporadic ALS/FTLD brains, the overwhelming majority of hippocampal dentate gyrus neurons containing TDP-43 inclusions were positive for p62 (Fig. 3A and B). TDP-43-positive/p62-positive neurons were also seen in the *C9orf72* hippocampus (Fig. 3A), but were much less abundant than in sporadic ALS/FTLD (Fig. 3A and B). There were numerous inclusions positive for p62 but negative for TDP-43 in *C9orf72* hippocampus, reminiscent of pathology in the cerebellum, but this pattern of staining was virtually absent in sporadic ALS/FTLD

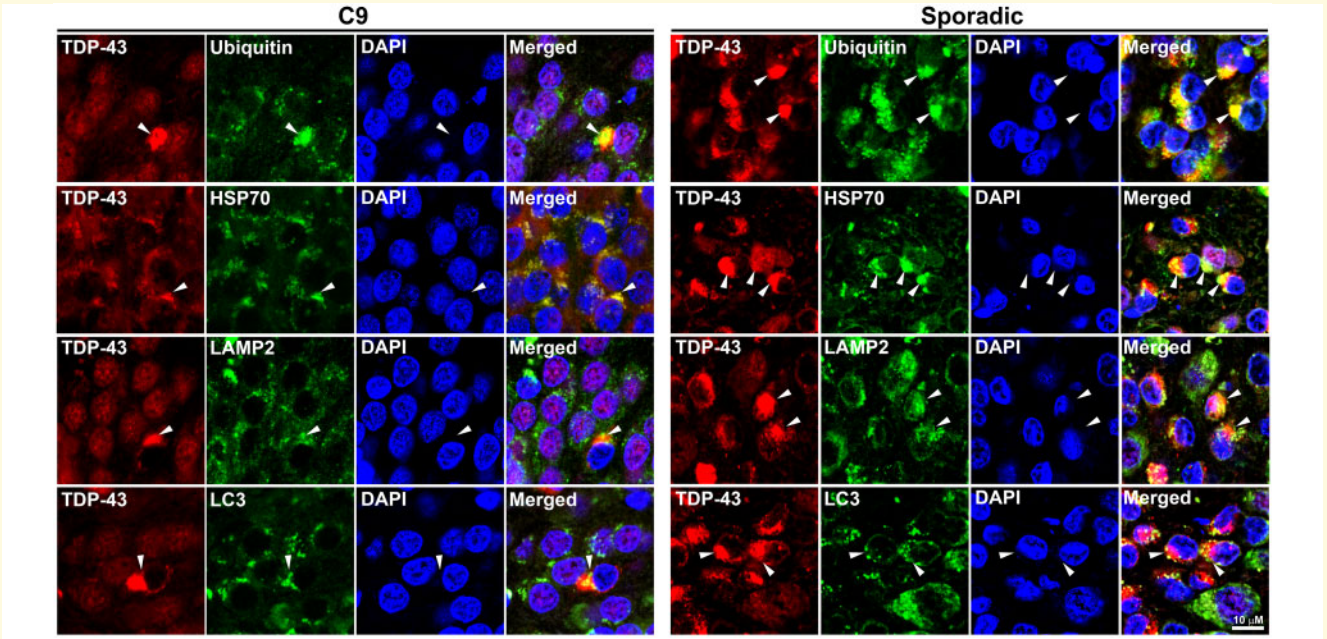

Figure 4 TDP-43 inclusions in *C9orf72* and sporadic ALS/FTLD hippocampus co-localized with ubiquitin and aggresome markers. Paraffin-embedded hippocampal sections from *C9orf72* or sporadic ALS/FTLD patients were subjected to double immunofluorescence histochemistry with antibodies against TDP-43 (red) and ubiquitin, HSP70, LAMP2 or LC3 (green). White arrowheads indicate examples of neurons with TDP-43 inclusions. Nuclei were visualized by DAPI stain (blue). C9, *C9orf72*; HSP70, heat shock protein 70 kDa; LAMP2, lysosomal-associated membrane protein 2.

(Fig. 3A and C). These findings in the *C9orf72* hippocampus, together with a complete lack of TDP-43 inclusions and an abundance of p62 inclusions in the cerebellum (Supplementary Fig. 1), indicate that TDP-43-negative/p62-positive inclusions are a pathological feature that distinguishes *C9orf72* ALS/FTLD from sporadic ALS/FTLD in hippocampus as well as in the cerebellum.

TDP-43 inclusions in sporadic and *C9orf72* ALS/FTLD are autophagy substrates

Additional double immunofluorescence analyses using the C-terminal TDP-43 antibody demonstrated that TDP-43 inclusions of various sizes in both sporadic and *C9orf72* ALS/FTLD hippocampi co-localized with ubiquitin (Fig. 4) which represents the deposition of ubiquitinated proteins, including TDP-43 (Neumann *et al.*, 2006; Richter-Landsberg and Leyk, 2013). In addition, the chaperone heat shock protein 70 kDa (HSP70), which is thought to protect neurons from toxicity of misfolded proteins (Turturici *et al.*, 2011), co-localized with TDP-43 inclusions in both sporadic and *C9orf72* ALS/FTLD hippocampus (Fig. 4, Supplementary Fig. 5). These TDP-43 inclusions also co-localized with and/or were surrounded by the autophagosome marker LC3 and the lysosome marker lysosome-associated membrane protein 2 (LAMP2; Fig. 4). Hippocampi from control patients did not demonstrate co-localization between TDP-43 and these markers (Supplementary Fig. 5). Thus, TDP-43 inclusions in sporadic and *C9orf72* ALS/FTLD share similar characteristics and are likely substrates for autophagy.

Sporadic and *C9orf72* ALS/FTLD patients have elevated TDP-43 protein levels in the frontal cortex and hippocampus

Whether TDP-43 protein levels are altered in sporadic and *C9orf72* ALS/FTLD brains has not been established. Immunoblotting of post-mortem frontal cortex and hippocampus demonstrated elevated TDP-43 levels in both sporadic and *C9orf72* ALS/FTLD patients as compared with controls (Fig. 5A and B, Supplementary Fig. 6), consistent with results from our recent proteomic analysis of frontal cortex tissues (Umoh *et al.*, 2018). The actin loading control did not show differences between sporadic and *C9orf72* ALS/FTLD patients and controls (Fig. 5A and B). TDP-43 protein levels did not differ between sporadic and *C9orf72* cases (Fig. 5A and B). Elevated levels of TDP-43 protein were not observed in clinically unaffected regions of the brain such as the cerebellum (Fig. 5C, Supplementary Fig. 6). Increased TDP-43 protein levels were also not seen in the frontal cortex and hippocampus of sporadic ALS patients without clinical FTD or pathological FTLD diagnoses (Supplementary Fig. 7).

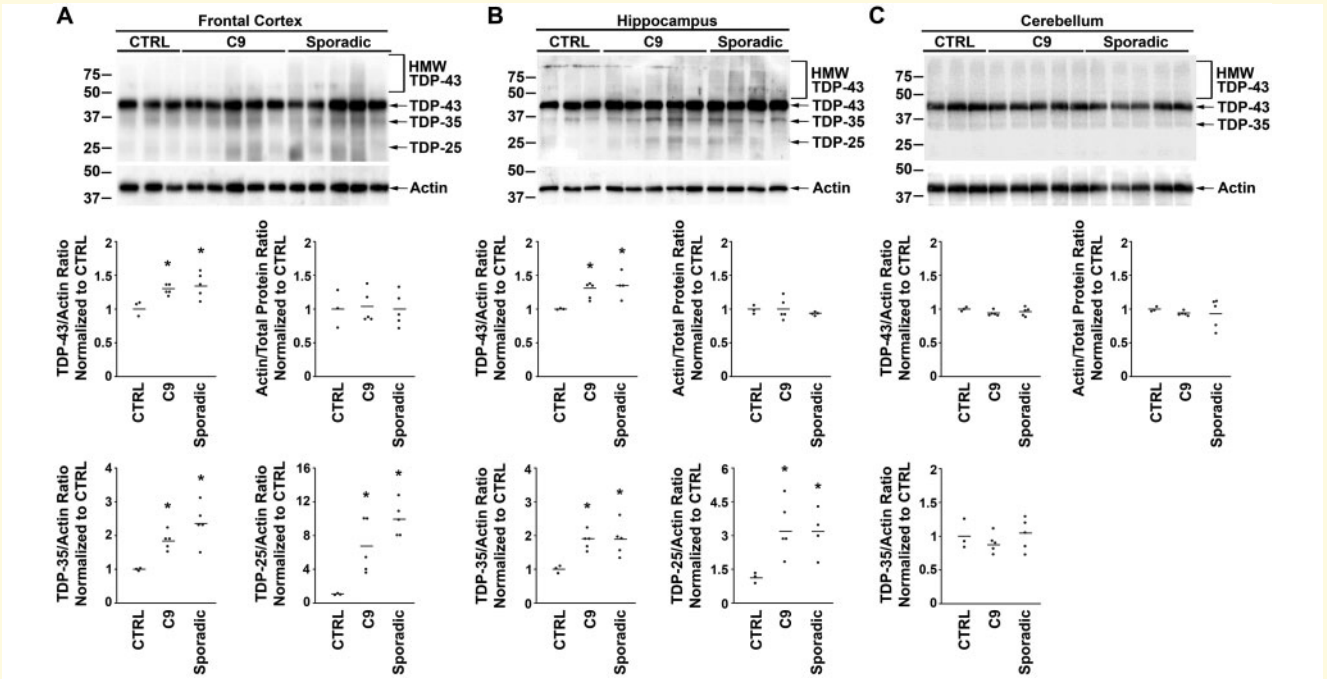

Figure 5 *C9orf72* and sporadic ALS/FTLD have increased TDP-43 protein levels in the frontal cortex and hippocampus. Equal amounts of total proteins from the indicated human patient frontal cortex (**A**), hippocampus (**B**) and cerebellum (**C**) were subjected to immunoblot analysis with anti-C-terminal TDP-43 antibody and anti-actin antibodies. The protein levels of full-length TDP-43 and the C-terminal fragments TDP-35 and TDP-25 were quantified and normalized to actin, and the protein levels of actin were quantified and normalized to total protein. The mean for each experimental group was represented by a horizontal line. Quantification of TDP-25 protein levels in the cerebellum was not provided due to absence of this species in the immunoblot. *$P < 0.05$ compared with control based on one-way ANOVA and post-hoc Tukey's test. C9, *C9orf72*; CTRL, control; HMW TDP-43, higher molecular weight species identified by the C-terminal anti-TDP-43 antibody.

Western blot analysis of sporadic and *C9orf72* ALS/FTLD also revealed the presence of lower molecular weight TDP-43 species in the frontal cortex (Fig. 5A) and hippocampus (Fig. 5B) that were significantly less prominent in controls and likely represent C-terminal fragments of TDP-43. Amongst these fragments, the protein bands at 35 kDa and at 25 kDa correspond to previously reported TDP-43 C-terminal fragments termed TDP-35 and TDP-25, respectively (Neumann *et al.*, 2006; Igaz *et al.*, 2008). TDP-25 is of particular interest as it was recently implicated to be cytotoxic (Yang *et al.*, 2010; Gregory *et al.*, 2012). These results suggest that excess TDP-43 in the frontal cortex and hippocampus is associated with the increased presence of potentially toxic C-terminal fragments that could contribute to the pathogenesis of sporadic and *C9orf72* ALS/FTLD.

Sporadic and *C9orf72* ALS/FTD fibroblasts demonstrate impairment in proteasomal degradation of TDP-43

The finding of elevated TDP-43 protein levels in both sporadic and *C9orf72* ALS/FTLD brains and the smaller TDP-43 inclusion size in *C9orf72* ALS/FTLD brains prompted us to further investigate these observations using an *in vitro* cellular model. Patient-derived fibroblasts from clinically diagnosed sporadic and *C9orf72* ALS/FTD patients show abnormally increased TDP-43 protein levels as compared with controls (Sabatelli *et al.*, 2015), which made this an attractive cellular model for studying how excess TDP-43 protein is processed in patient-derived cells. Note that the sporadic ALS/FTD fibroblasts were generated from living FTD patients who also had ALS, since the pathology of sporadic FTD in ALS patients is exclusively FTLD–TDP regardless of the clinical FTD subtype (Neumann *et al.*, 2006; Neumann *et al.*, 2007).

Our finding of excess TDP-43 protein in the frontal cortex and hippocampus of sporadic and *C9orf72* ALS/FTLD patients (Fig. 5) raised the possibility that TDP-43 turnover via the UPS may be impaired in these patients. To test this possibility, we first assessed the effects of proteasome inhibition on steady-state protein levels of TDP-43 in patient-derived fibroblasts (Fig. 6A, Supplementary Fig. 8A). Proteasome inhibition by MG132 had no effect on TDP-43 protein levels in sporadic and *C9orf72* ALS/FTD and ALS fibroblasts, suggesting that TDP-43 protein is not degraded by the UPS in fibroblasts from these patients (Fig. 6A and B). In contrast, proteasome inhibition significantly

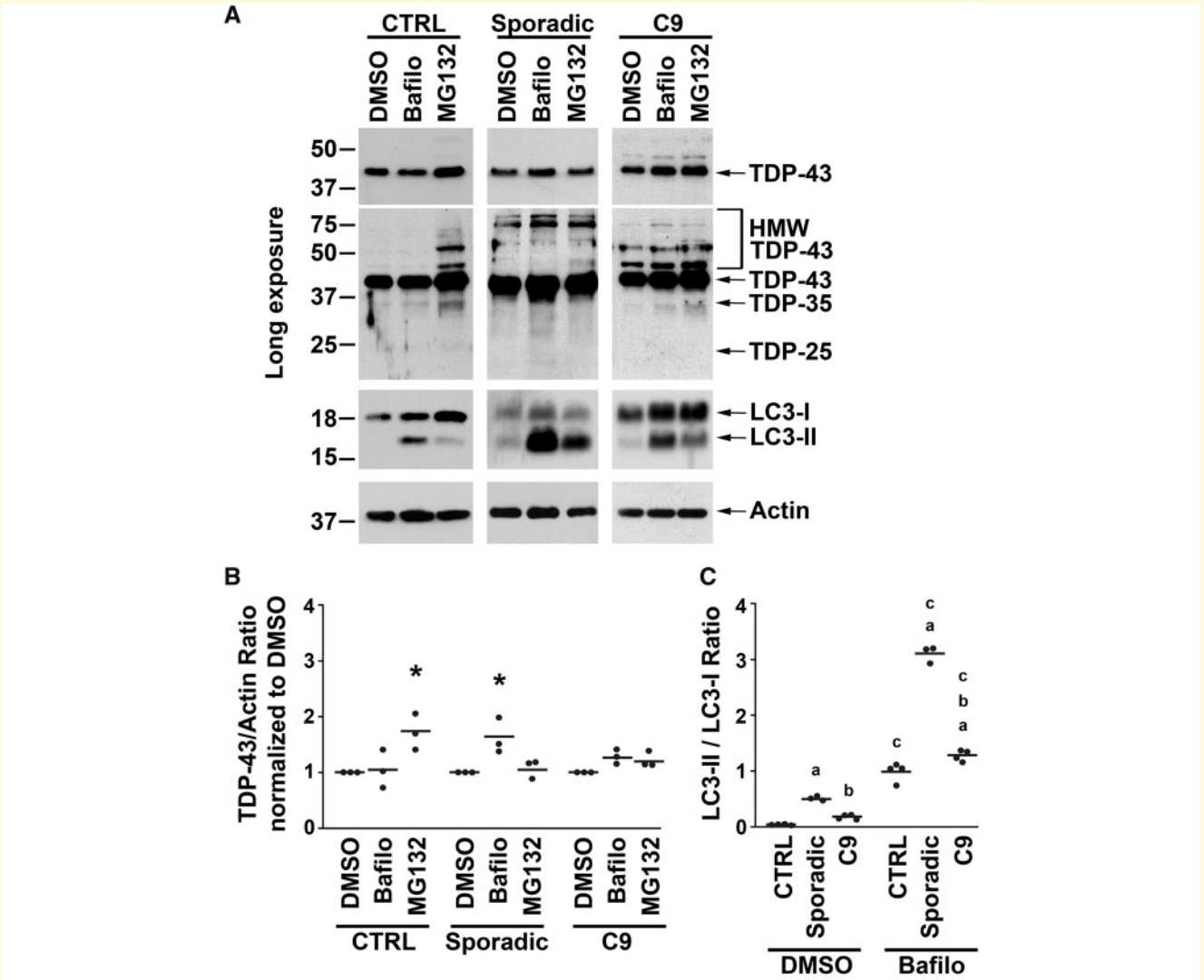

Figure 6 Sporadic and *C9orf72* disease fibroblasts showed proteasome impairment and autophagic degradation of TDP-43. (**A**) Patient-derived fibroblasts were treated for 24 h with 20 μM MG132, 50 nM of bafilomycin A1 (Bafilo) or vehicle control (DMSO). Equal amounts of total proteins from the indicated fibroblasts were subjected to immunoblot analysis with anti-C-terminal TDP-43, anti-actin and anti-LC3 antibodies. (**B**) The protein levels of full-length TDP-43 from control, sporadic and *C9orf72* ALS/FTD were quantified and normalized to vehicle treatment and to actin. The effects of MG132 and bafilomycin A1 on full-length TDP-43 protein level among control, sporadic and *C9orf72* ALS/FTD fibroblasts were shown. The mean for each experimental group was represented by a horizontal line.*$P < 0.05$ compared with the corresponding vehicle treatment group based on two-way ANOVA and post-hoc Tukey's test. (**C**) The ratios of LC3-II and LC3-I protein levels with vehicle treatment were compared between control, sporadic and *C9orf72* ALS/FTD fibroblasts. The mean for each experimental group was represented by a horizontal line. $^{a}P < 0.05$ when compared with the corresponding control fibroblasts, $^{b}P < 0.05$ when compared with the corresponding sporadic ALS/FTD fibroblasts, $^{c}P < 0.05$ when compared with the corresponding vehicle-treated fibroblasts based on two-way ANOVA and post-hoc Tukey's test. C9, *C9orf72*; CTRL, control; bafilo, bafilomycin A1; HMW TDP-43, higher molecular weight species identified by the C-terminal anti-TDP-43 antibody.

increased TDP-43 protein levels in control fibroblasts, indicating that TDP-43 is normally degraded by the UPS (Fig. 6A and B). In addition, HMW TDP-43 species were seen in vehicle-treated sporadic and *C9orf72* disease fibroblasts but were only found in control fibroblasts after proteasome inhibition with MG132 (Fig. 6A), indicating that HMW species likely represent accumulation of ubiquitinated TDP-43. Proteasome inhibition by MG132 also had no effect on poly-ubiquitinated protein levels in sporadic and *C9orf72* disease fibroblasts, suggesting the inability of the proteasome pathway to degrade poly-ubiquitinated proteins in these fibroblasts (Supplementary Fig. 8B and C). Together, these findings suggest that TDP-43 degradation via the proteasome pathway is impaired in both sporadic and *C9orf72* disease fibroblasts which could be responsible for the accumulation of TDP-43 protein in ALS/FTLD brains.

Sporadic ALS/FTD fibroblasts degrade TDP-43 via autophagy more effectively than *C9orf72* fibroblasts

When the UPS fails, proteins such as TDP-43 have the potential to form oligomers which are small protein aggregates (Ross and Poirier, 2005; Johnson *et al.*, 2009). Aggregated proteins are cleared by the autophagy pathway where autophagosomes engulf these aggregates and then fuse with lysosomes to eliminate them via enzymatic degradation (Klionsky *et al.*, 2012). Autophagy activation causes the conversion of LC3-I to LC3-II, and LC3-II is subsequently degraded by autophagy (Klionsky *et al.*, 2012). We first examined whether there was a difference in autophagy activation by studying LC3 conversion in these fibroblasts. Our results show that LC3-II/LC3-I ratio is low in control fibroblasts and is significantly higher in both sporadic and *C9orf72* disease fibroblasts (Fig. 6A and C, Supplementary Fig. 8). To see whether this increase in LC3-II/LC3-I ratio in sporadic and *C9orf72* ALS/FTD and ALS fibroblasts resulted from autophagy activation or from impairment of autophagic degradation and subsequent build-up of LC3-II, we treated fibroblasts with the autophagy inhibitor bafilomycin A1. Bafilomycin A1 treatment resulted in further increase in the LC3-II/LC3-I ratio in sporadic and *C9orf72* disease fibroblasts, indicating that autophagy degradation of LC3-II was intact in these cells (Fig. 6A and C). Therefore, it is likely that the increased LC3-II/LC3-I ratio in sporadic and *C9orf72* disease fibroblasts compared with control fibroblasts reflects an activation of autophagy in sporadic and *C9orf72*-associated disease.

We examined the effects of bafilomycin A1 on TDP-43 protein levels and found that it raised TDP-43 protein levels in sporadic disease fibroblasts (Fig. 6A and B). A trend towards an increase in TDP-43 protein levels in *C9orf72* cells did not reach statistical significance (Fig. 6A and B). These findings suggest that although UPS is impaired in both sporadic and *C9orf72* disease fibroblasts, the autophagy pathway is responsible for degrading TDP-43 in these fibroblasts and further implies that autophagic degradation of TDP-43 may be more robust in sporadic cases compared with *C9orf72* cases.

Proteasome inhibition causes TDP-43 aggresome formation in sporadic ALS/FTD but not in *C9orf72* fibroblasts

The pTDP-43 inclusions were not seen in vehicle-treated sporadic ALS/FTD fibroblasts (Fig. 7A), but proteasome inhibition with MG132 resulted in pTDP-43 accumulation in inclusion bodies (Fig. 7A). These findings are consistent with prior studies demonstrating the induction of TDP-43 phoshorylation by MG132 in cells (Nonaka *et al.*, 2009; van Eersel *et al.*, 2011). The perinuclear location of these inclusions suggested that they might be aggresomes. Aggresome formation is a cellular response that occurs when the capacity of the proteasome is exceeded by the production of misfolded and/or toxic proteins (Johnston *et al.*, 1998). Aggresomes can also be induced by proteasome inhibition (Richter-Landsberg and Leyk, 2013). Cells target toxic proteins to perinuclear aggresomes via microtubule-dependent retrograde transport and sequester these proteins by encapsulating them with vimentin intermediate filaments or neurofilaments (Johnston *et al.*, 1998). The pTDP-43 inclusion bodies in MG132-treated fibroblasts were caged by vimentin and also were enriched with ubiquitin, HSP70, p62, LC3, LAMP2, defining them as aggresomes (Fig. 7A and B). Further proof that these pTDP-43 inclusions were aggresomes comes from the demonstration that they did not co-localize with the Golgi apparatus marker GM130 nor the mitochondrial marker TIM23 but juxtaposed the endoplasmic reticulum marker KDEL (Supplementary Fig. 9), all of which are known features of aggresomes (Kopito and Sitia, 2000; Walker *et al.*, 2013). Treatment with nocodazole, a microtubule-depolymerizing drug, abolished the pTDP-43 inclusions providing further confirmation that these were *bona fide* aggresomes (Fig. 7B).

Our finding of the reduced abundance of TDP-43 inclusions and the presence of soluble cytoplasmic TDP-43 in *C9orf72* ALS/FTLD brains (Figs. 1 and 2) suggested that the *C9orf72* mutation may inhibit the formation of insoluble TDP-43 inclusions. To test this possibility *in vitro*, we examined patient-derived fibroblasts under the condition of proteasome inhibition with MG132. Treatment with MG132 resulted in increased pTDP-43 levels and the formation of large pTDP-43 positive inclusions in sporadic ALS/FTD and ALS fibroblasts but to a lesser degree in *C9orf72* fibroblasts (Fig. 8A and B). However, p62 levels were similar in sporadic and *C9orf72* fibroblasts (Fig. 8A and C). As these aggresomes were both pTDP-43 and p62-positive (Fig. 7A and B), we measured the formation of pTDP-43 aggresomes by examining pTDP-43 co-localization with p62. We found a reduced pTDP-43 co-localization with p62-positive aggresomes in *C9orf72* fibroblasts compared with sporadic disease fibroblasts (Fig. 8A and D), indicating that *C9orf72* fibroblasts were impaired in their ability to form pTDP-43 aggresomes. The reduced pTDP-43 inclusion formation and lack of pTDP-43/p62 co-localization in *C9orf72* patient fibroblasts were consistent with our observations in *C9orf72* and sporadic ALS/FTLD brains (Figs. 1 and 3).

Using the C-terminal TDP-43 antibody to examine other forms of TDP-43, we found that TDP-43 immunostaining overlapped with the nuclear staining marker DAPI in vehicle-treated control fibroblasts (Fig. 8E and F). However, in vehicle-treated *C9orf72* fibroblasts, TDP-43 immunostaining was found in the cytoplasm with reduced nuclear TDP-43 signal as compared with

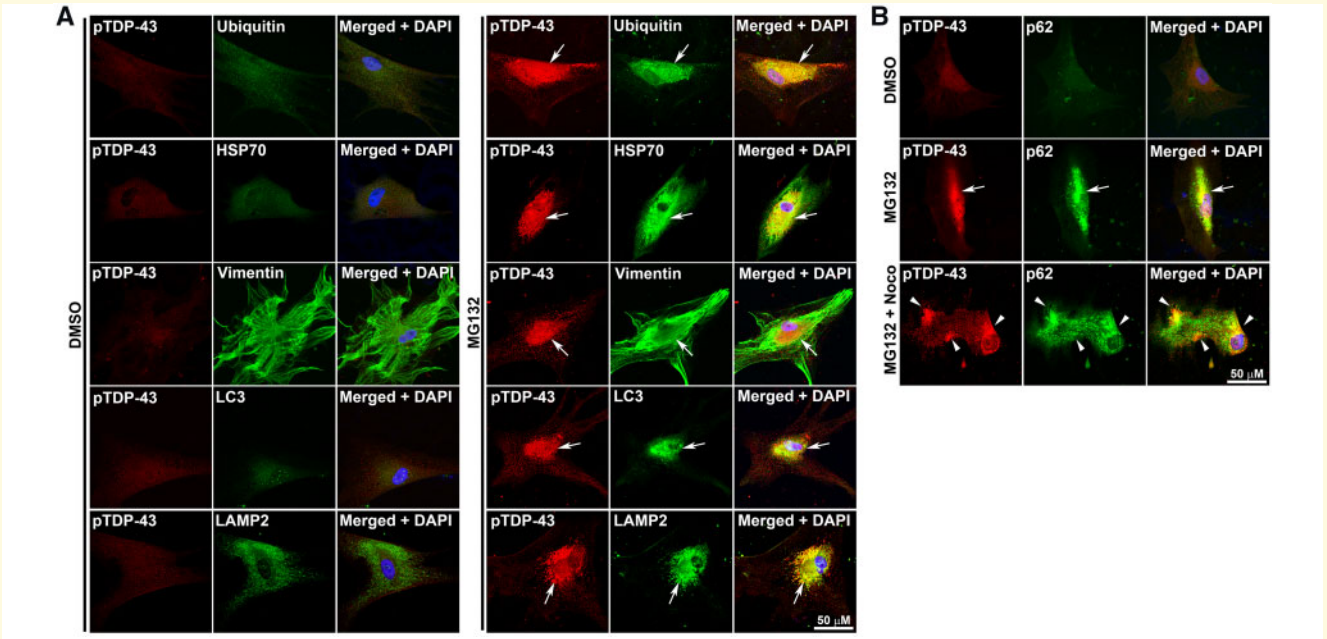

Figure 7 Proteasome impairment induced the formation of pTDP-43 aggresomes in sporadic ALS/FTD fibroblasts. (**A**) Fibroblasts from sporadic ALS/FTD were treated for 24 h with 20 μM MG132 or vehicle control (DMSO) and then immunostained with pTDP-43 (red) and ubiquitin, HSP70, vimentin, LC3 or LAMP2 (green) antibodies. (**B**) Formation of pTDP-43 aggresome was microtubule-dependent. Fibroblasts from sporadic ALS/FTD were treated for 24 h with vehicle control, 20 μM MG132, or 20 μM MG132 plus 2 μg/ml nocodazole (Noco) for 24 h and were immunostained with anti-pTDP-43 (red) and anti-p62 (green) antibodies. Nuclei were visualized by DAPI stain (blue). Aggresomes were indicated by white arrows. pTDP-43 microaggregates were indicated by white arrow heads. HSP70, heat shock protein 70 kDa; LAMP2, lysosomal-associated membrane protein 2; noco, nocodazole; pTDP-43, phosphorylated TDP-43.

fibroblasts from controls (Fig. 8E and F). A similar pattern of TDP-43 staining was seen in vehicle-treated sporadic disease fibroblasts but was not statistically significant (Fig. 8E and F). Proteasome inhibition again resulted in formation of TDP-43-positive/p62-positive aggresomes in sporadic disease fibroblasts that were reduced in *C9orf72* fibroblasts (Fig. 8E, G, and H, Supplementary Fig. 10). Rather than being sequestered to the aggresome, TDP-43 accumulated as diffuse cytoplasmic staining in *C9orf72* fibroblasts (Fig. 8E and F, Supplementary Fig. 10).

Discussion

The current study identified several major pathological differences in TDP-43 inclusion formation between sporadic and *C9orf72*-related disease patients. We confirmed in our pathological samples the previously reported TDP-43-negative/p62-positive inclusions in the cerebellum and hippocampus that define *C9orf72* ALS/FTLD neuropathology (Al-Sarraj *et al.*, 2011; Troakes *et al.*, 2012). In these cases, the hippocampi from sporadic ALS/FTLD contained numerous and easily identified circumferential and round pTDP-43 inclusions, whereas pTDP-43 inclusions were proportionally fewer and were morphologically smaller in *C9orf72* ALS/FTLD hippocampi. These findings are consistent with two recently published reports on *C9orf72* cases without robust TDP-43 pathology (Vatsavayai *et al.*, 2016; Nana *et al.*, 2019). Another important finding was the demonstration of soluble cytoplasmic TDP-43 in *C9orf72* ALS/FTLD that was largely absent in sporadic ALS/FTLD. Both sporadic and *C9orf72* brains had similarly elevated TDP-43 protein levels in the frontal cortex and hippocampus; therefore, the differences in TDP-43 inclusion body formation between sporadic and *C9orf72*-related diseases could not be attributed to a difference in TDP-43 protein abundance. The lesser presence of TDP-43 inclusions in *C9orf72* neurons cannot be attributed to a generalized reduced ability to form cytoplasmic inclusion bodies, as p62 inclusions are more abundant in the *C9orf72* hippocampus than sporadic cases. The presence of cytosolic TDP-43 protein in *C9orf72* ALS/FTLD neurons is not surprising given recent studies indicating that the nucleocytoplasmic transport of TDP-43 is impaired in *Drosophila* and neuronal culture models of *C9orf72*-related disease (Zhang *et al.*, 2015; Khosravi *et al.*, 2017). We suggest that the presence of soluble TDP-43 protein in the cytoplasm of *C9orf72* ALS/FTLD neurons, together with the smaller sizes and proportionally fewer TDP-43 inclusions in these neurons, might implicate an impairment of cytoplasmic TDP-43 inclusion body formation in *C9orf72* patients *in vivo*. Supporting this conclusion are the experiments in

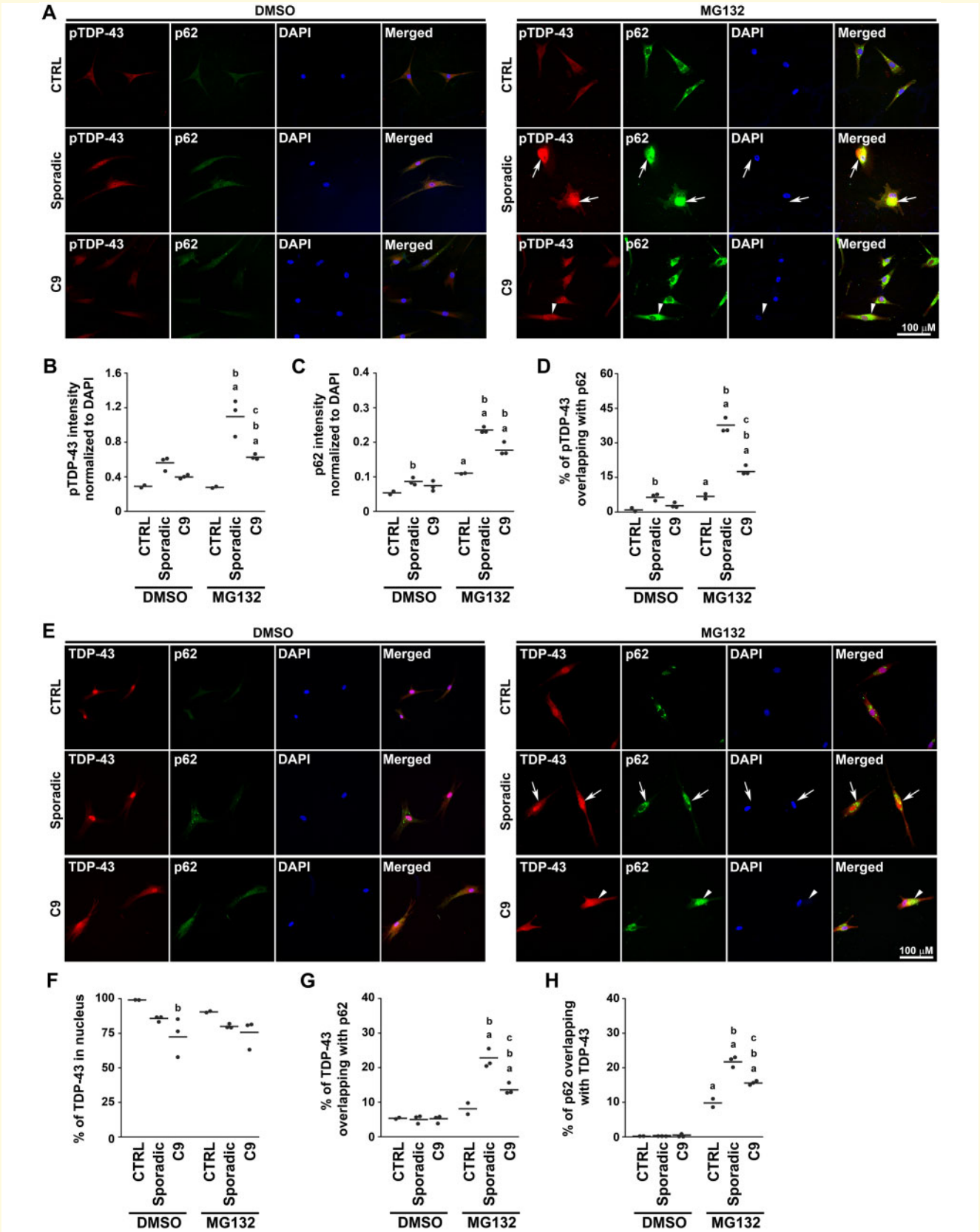

Figure 8 Targeting of TDP-43 to aggresomes was impaired in *C9orf72* fibroblasts. (**A**) Human patient-derived fibroblasts were treated for 24 h with 20 μM MG132 or vehicle control (DMSO) and then immunostained with phospho-TDP-43 (pTDP-43, red) and p62 (green) antibodies. Examples of pTDP-43-positive/p62-positive aggresomes were indicated by white arrows. Examples of areas where pTDP-43 had some co-localization with p62 were indicated by white arrow heads. Nuclei were visualized by DAPI stain (blue). (**B**, **C**) The intensity of

patient-derived fibroblasts, which revealed that the induction of microtubule-dependent TDP-43 inclusion body formation by proteasome inhibition was deficient in *C9orf72* fibroblasts compared with sporadic disease fibroblasts. Taken together, these data from ALS/FTLD brains and patient-derived fibroblasts demonstrate that turnover of TDP-43 protein is handled differently in *C9orf72*-related diseases, and suggests that there is an impairment of TDP-43 inclusion body formation in *C9orf72* patients compared with sporadic disease patients.

The abnormal HRE in *C9orf72* is transcribed bidirectionally to form nuclear RNA foci (DeJesus-Hernandez *et al.*, 2011; Wojciechowska and Krzyzosiak, 2011) and is translated in an AUG-independent manner from both sense and antisense *C9orf72* transcripts into five distinct dipeptide protein repeats (Mann *et al.*, 2013; Mori *et al.*, 2013). These distinct dipeptide protein repeats form neuronal cytoplasmic inclusions that stain positive for p62 (Mann *et al.*, 2013; Mori *et al.*, 2013). The fact that *C9orf72* ALS/FTLD was uniquely characterized by TDP-43-negative/p62-positive inclusions, together with the presence of distinct dipeptide protein repeats-positive/p62-positive inclusions, suggest a possibility that distinct dipeptide protein repeats might compete with TDP-43 to become the major constituent of inclusion bodies in *C9orf72* patients. It is also possible that RNA foci could block the formation of TDP-43 inclusions via unknown mechanisms. In addition, the abnormal HRE in *C9orf72* causes haploinsufficiency in the *C9orf72* protein which could affect protein quality control systems (Burk and Pasterkamp, 2019) to disrupt TDP-43 inclusion body formation. Another possible reason for impaired TDP-43 inclusion body formation could be that the *C9orf72* mutation, via yet-to-be-identified mechanisms, inhibits the phosphorylation of TDP-43 to block the targeting of TDP-43 into inclusion bodies (Brady *et al.*, 2011). This hypothesis is supported by our findings that the diffuse cytoplasmic soluble TDP-43 in *C9orf72* patient-derived fibroblasts was not labelled by the anti-phospho-TDP-43 antibody and thus represents non-phosphorylated forms of TDP-43. Why the presence of diffuse cytosolic TDP-43 was not always associated with TDP-43 nuclear clearing, which is typically seen in neurons with TDP-43 cytoplasmic inclusions, is unknown, but may have to do with different degree of nucleocytoplasmic transport dysfunction in these *C9orf72* neurons. Additional studies are needed to investigate the possible mechanisms underlying how the *C9orf72* mutation inhibits the targeting of TDP-43 into inclusion bodies and dysregulates nucleocytoplasmic transport of TDP-43, which could have important implications in understanding the pathogenesis of *C9orf72*-related TDP-43 proteinopathies such as FTD and ALS.

Our observation of excess TDP-43 protein and its toxic C-terminal fragments in the frontal cortex and hippocampus of sporadic and *C9orf72* ALS/FTLD, together with previous studies showing that an overabundance of TDP-43 protein causes neurotoxicity and ALS/FTLD phenotype and pathology in transgenic mice (Wils *et al.*, 2010; Igaz *et al.*, 2011), provides strong evidence to suggest that aberrantly increased TDP-43 protein levels may contribute to sporadic and *C9orf72* ALS/FTLD pathogenesis, possibly via a toxic gain-of-function mechanism. In support of this mechanistic hypothesis is that elevated TDP-43 protein levels in the frontal cortex and hippocampus were seen only in the patients with FTD and pathological FTLD, but TDP-43 protein levels in non-demented, sporadic ALS patients were the same as controls. In addition, our previous work using quantitative proteomics also demonstrated elevated levels of TDP-43 in the frontal cortex of FTD patients as compared with controls (Umoh *et al.*, 2018).

Our *in vitro* studies demonstrated that TDP-43 degradation by the UPS is impaired in sporadic and *C9orf72* ALS/FTD fibroblasts, which might explain the abnormal accumulation of TDP-43 protein in both patient-derived ALS/FTD fibroblasts (Sabatelli *et al.*, 2015) and ALS/FTLD brains. The selectively increased TDP-43 protein levels in clinically affected brain regions in ALS/FTLD (frontal cortex and hippocampus), but not in relatively unaffected areas (cerebellum), raises the possibility that the dysfunction in proteasome degradation of TDP-43 correlates with clinical disease activity. Why elevation of TDP-43 protein levels associated with sporadic and *C9orf72* ALS/FTD is found in fibroblasts without known skin manifestations in these patients remains unknown. One possibility is that certain brain regions are more vulnerable to TDP-43 toxicity, which is supported by a transgenic mouse model expressing human TDP-43 in all

Figure 8 Continued

pTDP-43 (**B**) and p62 (**C**) immunostaining in patient fibroblasts was normalized to DAPI intensity and quantified as described in Materials and Methods section. (**D**) The percentages of pTDP-43 co-localized with p62 in patient fibroblasts were quantified as described in the Materials and Methods section. (**E**) Human patient-derived fibroblasts were treated for 24 h with 20 μM MG132 or vehicle control (DMSO) and then immunostained with C-terminal TDP-43 (TDP-43, red) and p62 (green) antibodies. Examples of TDP-43-positive aggresomes were indicated by white arrows. Examples of areas where TDP-43 had some co-localization with p62 were indicated by white arrow heads. Nuclei were visualized by DAPI stain (blue). The percentages of TDP-43 co-localized with nucleus as visualized by DAPI stain (**F**), TDP-43 co-localized with p62 (**G**) and p62 co-localized with TDP-43 (**H**) were quantified as described in the Materials and Methods section. All statistical analyses in this figure were carried out using each case as the experimental unit as described in the Materials and Methods section. The mean for each experimental group was represented by a horizontal line. $^{a}P < 0.05$ when compared with the corresponding vehicle-treated fibroblasts, $^{b}P < 0.05$ when compared with the corresponding control fibroblasts, $^{c}P < 0.05$ when compared with the corresponding sporadic disease fibroblasts based on two-way ANOVA and post-hoc Tukey's test. C9, *C9orf72*; CTRL, control; pTDP-43, phosphorylated TDP-43.

tissues but only demonstrating central nervous system manifestation and pathology without causing disease in other organs (Swarup *et al.*, 2011). In the setting of proteasome inhibition, sporadic ALS/FTD fibroblasts formed TDP-43 aggresomes that were tightly associated with autophagosomes and lysosomes. This finding is consistent with numerous reports that suggest aggresomes are staging areas for the degradation of misfolded proteins by autophagy (Iwata *et al.*, 2005*a*, *b*; Mehrpour *et al.*, 2010; Lee *et al.*, 2011) and may explain why aggresome formation is not associated with increased protein levels in cells (Zaarur *et al.*, 2008). Several studies have reported that aggresome formation correlates with cell survival (Kawaguchi *et al.*, 2003; Taylor *et al.*, 2003; Shiarli *et al.*, 2006). TDP-43 aggresomes in fibroblasts resembled the TDP-43 cytoplasmic neuronal inclusions in ALS/FTLD brains in that they were both perinuclear in location and that they co-localized with ubiquitin, p62 and HSP70. These inclusions also co-localized with autophagosomes and lysosomes and, therefore, likely served as a location for degradation of excess TDP-43 protein by autophagy.

TDP-43 aggresome formation in response to proteasome inhibition was impaired in *C9orf72* fibroblasts compared with sporadic disease fibroblasts. The inability to consolidate TDP-43 into aggresomes likely resulted in inefficient autophagic degradation of excess TDP-43, which suggested an impairment of protein quality control responses and increased cellular toxicity in *C9orf72*-related diseases. Despite a conundrum in the neurodegenerative disease literature regarding whether soluble protein oligomers or insoluble protein inclusions are the culprits for neurotoxicity, the general consensus is that the sequestration of soluble aggregated toxic proteins including TDP-43 by active microtubule-dependent mechanisms into insoluble aggregates is beneficial by preventing toxic, misfolded proteins from saturating chaperones and the proteasome and facilitating their clearance via autophagy (Ross and Poirier, 2004; Cohen *et al.*, 2006; Scotter *et al.*, 2014; Sontag *et al.*, 2014; Sweeney *et al.*, 2017; Soto and Pritzkow, 2018). Supporting this view, several studies have reported that aggresome formation correlates with cell survival (Kawaguchi *et al.*, 2003; Taylor *et al.*, 2003; Shiarli *et al.*, 2006). Our study of mutant SOD1 proteins also showed that soluble mutant proteins were demonstrable only in pathologically affected spinal cord tissues, further suggesting that soluble protein species are responsible for ALS pathogenesis (Brotherton *et al.*, 2012). However, cells are known to be dynamic creatures that can form insoluble proteins from soluble proteins (Bagola and Sommer, 2008) and, therefore, it is virtually impossible to purely isolate and test which protein species mediate cytotoxicity.

The demonstration of aggresome formation in the current work is a cell culture phenomenon that does not necessarily represent the inclusion bodies found in brains. It is also unclear whether the impairment of TDP-43 inclusion body formation in *C9orf72* patients has clinical significance given that there are no major phenotypic differences between *C9orf72* and sporadic ALS/FTLD patients. Furthermore, impairment of protein quality control systems in these patients could affect not only TDP-43 but also other potentially toxic proteins to contribute to disease pathogenesis. Future studies are needed to determine the clinical and pathophysiological significances of these findings.

Supplementary material

Supplementary material is available at *Brain Communications* online.

Acknowledgements

We thank the Emory University Alzheimer Disease Research Center (ADRC) for providing central nervous system tissue samples and the patient family members who contributed those tissues. We also thank Emory University School of Medicine Neurology Residency Training Program for providing 6 months of protected research time for S.M.L.

Funding

This work was supported in part by National Institutes of Health grants (AG025688 to J.D.G. and M.G., NS055077 to M.G., NS092343 to L.L., NS093550 to L.S.C. and K08-NS087121 to C.M.H.) and by research funding from the Amyotrophic Lateral Sclerosis Association and the Muscular Dystrophy Association.

Competing interests

The authors report no competing interests.

References

Aber KM, Nori P, MacDonald SM, Bibat G, Jarrar MH, Kaufmann WE. Methyl-CpG-binding protein 2 is localized in the postsynaptic compartment: an immunochemical study of subcellular fractions. Neuroscience 2003; 116: 77–80.

Al-Kofahi Y, Lassoued W, Lee W, Roysam B. Improved automatic detection and segmentation of cell nuclei in histopathology images. IEEE Trans Biomed Eng 2010; 57: 841–52.

Al-Sarraj S, King A, Troakes C, Smith B, Maekawa S, Bodi I, et al. p62 positive, TDP-43 negative, neuronal cytoplasmic and intranuclear inclusions in the cerebellum and hippocampus define the pathology of C9orf72-linked FTLD and MND/ALS. Acta Neuropathol 2011; 122: 691–702.

Bagola K, Sommer T. Protein quality control: on IPODs and other JUNQ. Curr Biol 2008; 18: R1019–21.

Bigio EH, Weintraub S, Rademakers R, Baker M, Ahmadian SS, Rademaker A, et al. Frontotemporal lobar degeneration with TDP-43 proteinopathy and chromosome 9p repeat expansion in

C9ORF72: clinicopathologic correlation. Neuropathology 2013; 33: 122–33.

Blokhuis AM, Groen EJ, Koppers M, van den Berg LH, Pasterkamp RJ. Protein aggregation in amyotrophic lateral sclerosis. Acta Neuropathol 2013; 125: 777–94.

Brady OA, Meng P, Zheng Y, Mao Y, Hu F. Regulation of TDP-43 aggregation by phosphorylation and p62/SQSTM1. J Neurochem 2011; 116: 248–59.

Brettschneider J, Arai K, Del Tredici K, Toledo JB, Robinson JL, Lee EB, et al. TDP-43 pathology and neuronal loss in amyotrophic lateral sclerosis spinal cord. Acta Neuropathol 2014; 128: 423–37.

Brotherton TE, Li Y, Cooper D, Gearing M, Julien JP, Rothstein JD, et al. Localization of a toxic form of superoxide dismutase 1 protein to pathologically affected tissues in familial ALS. Proc Natl Acad Sci USA 2012; 109: 5505–10.

Burk K, Pasterkamp RJ. Disrupted neuronal trafficking in amyotrophic lateral sclerosis. Acta Neuropathol 2019; 137: 859–77.

Cairns NJ, Bigio EH, Mackenzie IR, Neumann M, Lee VM, Hatanpaa KJ, et al. Neuropathologic diagnostic and nosologic criteria for frontotemporal lobar degeneration: consensus of the Consortium for Frontotemporal Lobar Degeneration. Acta Neuropathol 2007; 114: 5–22.

Ciechanover A. The ubiquitin-proteasome proteolytic pathway. Cell 1994; 79: 13–21.

Cohen E, Bieschke J, Perciavalle RM, Kelly JW, Dillin A. Opposing activities protect against age-onset proteotoxicity. Science 2006; 313: 1604–10.

DeJesus-Hernandez M, Mackenzie IR, Boeve BF, Boxer AL, Baker M, Rutherford NJ, et al. Expanded GGGGCC hexanucleotide repeat in noncoding region of C9ORF72 causes chromosome 9p-linked FTD and ALS. Neuron 2011; 72: 245–56.

Giles LM, Chen J, Li L, Chin LS. Dystonia-associated mutations cause premature degradation of torsinA protein and cell-type-specific mislocalization to the nuclear envelope. Hum Mol Genet 2008; 17: 2712–22.

Gregory JM, Barros TP, Meehan S, Dobson CM, Luheshi LM. The aggregation and neurotoxicity of TDP-43 and its ALS-associated 25 kDa fragment are differentially affected by molecular chaperones in Drosophila. PLoS One 2012; 7: e31899.

Hinz FI, Geschwind DH. Molecular genetics of neurodegenerative dementias. Cold Spring Harb Perspect Biol 2017; 9: a023705.

Igaz LM, Kwong LK, Lee EB, Chen-Plotkin A, Swanson E, Unger T, et al. Dysregulation of the ALS-associated gene TDP-43 leads to neuronal death and degeneration in mice. J Clin Invest 2011; 121: 726–38.

Igaz LM, Kwong LK, Xu Y, Truax AC, Uryu K, Neumann M, et al. Enrichment of C-terminal fragments in TAR DNA-binding protein-43 cytoplasmic inclusions in brain but not in spinal cord of frontotemporal lobar degeneration and amyotrophic lateral sclerosis. Am J Pathol 2008; 173: 182–94.

Iwata A, Christianson JC, Bucci M, Ellerby LM, Nukina N, Forno LS, et al. Increased susceptibility of cytoplasmic over nuclear polyglutamine aggregates to autophagic degradation. Proc Natl Acad Sci USA 2005a; 102: 13135–40.

Iwata A, Riley BE, Johnston JA, Kopito RR. HDAC6 and microtubules are required for autophagic degradation of aggregated huntingtin. J Biol Chem 2005b; 280: 40282–92.

Johnson BS, Snead D, Lee JJ, McCaffery JM, Shorter J, Gitler AD. TDP-43 is intrinsically aggregation-prone, and amyotrophic lateral sclerosis-linked mutations accelerate aggregation and increase toxicity. J Biol Chem 2009; 284: 20329–39.

Johnston JA, Ward CL, Kopito RR. Aggresomes: a cellular response to misfolded proteins. J Cell Biol 1998; 143: 1883–98.

Kawaguchi Y, Kovacs JJ, McLaurin A, Vance JM, Ito A, Yao TP. The deacetylase HDAC6 regulates aggresome formation and cell viability in response to misfolded protein stress. Cell 2003; 115: 727–38.

Khosravi B, Hartmann H, May S, Mohl C, Ederle H, Michaelsen M, et al. Cytoplasmic poly-GA aggregates impair nuclear import of TDP-43 in C9orf72 ALS/FTLD. Hum Mol Genet 2017; 26: 790–800.

Klionsky DJ, Abdalla FC, Abeliovich H, Abraham RT, Acevedo-Arozena A, Adeli K, et al. Guidelines for the use and interpretation of assays for monitoring autophagy. Autophagy 2012; 8: 445–544.

Konrad C, Kawamata H, Bredvik KG, Arreguin AJ, Cajamarca SA, Hupf JC, et al. Fibroblast bioenergetics to classify amyotrophic lateral sclerosis patients. Mol Neurodegener 2017; 12: 76.

Kopito RR, Sitia R. Aggresomes and Russell bodies. Symptoms of cellular indigestion? EMBO Rep 2000; 1: 225–31.

Kreiling JA, Tamamori-Adachi M, Sexton AN, Jeyapalan JC, Munoz-Najar U, Peterson AL, et al. Age-associated increase in heterochromatic marks in murine and primate tissues. Aging Cell 2011; 10: 292–304.

Lee SM, Chin LS, Li L. Charcot-Marie-Tooth disease-linked protein SIMPLE functions with the ESCRT machinery in endosomal trafficking. J Cell Biol 2012; 199: 799–816.

Lee SM, Olzmann JA, Chin LS, Li L. Mutations associated with Charcot-Marie-Tooth disease cause SIMPLE protein mislocalization and degradation by the proteasome and aggresome-autophagy pathways. J Cell Sci 2011; 124 (Pt 19): 3319–31.

Mackenzie IR, Baborie A, Pickering-Brown S, Du Plessis D, Jaros E, Perry RH, et al. Heterogeneity of ubiquitin pathology in frontotemporal lobar degeneration: classification and relation to clinical phenotype. Acta Neuropathol 2006; 112: 539–49.

Mackenzie IR, Munoz DG, Kusaka H, Yokota O, Ishihara K, Roeber S, et al. Distinct pathological subtypes of FTLD-FUS. Acta Neuropathol 2011a; 121: 207–18.

Mackenzie IR, Neumann M, Baborie A, Sampathu DM, Du Plessis D, Jaros E, et al. A harmonized classification system for FTLD-TDP pathology. Acta Neuropathol 2011b; 122: 111–3.

Mann DM, Rollinson S, Robinson A, Bennion Callister J, Thompson JC, Snowden JS, et al. Dipeptide repeat proteins are present in the p62 positive inclusions in patients with frontotemporal lobar degeneration and motor neurone disease associated with expansions in C9ORF72. Acta Neuropathol Commun 2013; 1: 68.

Mehrpour M, Esclatine A, Beau I, Codogno P. Overview of macroautophagy regulation in mammalian cells. Cell Res 2010; 20: 748–62.

Misztal K, Brozko N, Nagalski A, Szewczyk LM, Krolak M, Brzozowska K, et al. TCF7L2 mediates the cellular and behavioral response to chronic lithium treatment in animal models. Neuropharmacology 2017; 113: 490–501.

Mori K, Weng SM, Arzberger T, May S, Rentzsch K, Kremmer E, et al. The C9orf72 GGGGCC repeat is translated into aggregating dipeptide-repeat proteins in FTLD/ALS. Science 2013; 339: 1335–8.

Nana AL, Sidhu M, Gaus SE, Hwang JL, Li L, Park Y, et al. Neurons selectively targeted in frontotemporal dementia reveal early stage TDP-43 pathobiology. Acta Neuropathol 2019; 137: 27–46.

Neumann M, Kwong LK, Sampathu DM, Trojanowski JQ, Lee VM. TDP-43 proteinopathy in frontotemporal lobar degeneration and amyotrophic lateral sclerosis: protein misfolding diseases without amyloidosis. Arch Neurol 2007; 64: 1388–94.

Neumann M, Sampathu DM, Kwong LK, Truax AC, Micsenyi MC, Chou TT, et al. Ubiquitinated TDP-43 in frontotemporal lobar degeneration and amyotrophic lateral sclerosis. Science 2006; 314: 130–3.

Nonaka T, Arai T, Buratti E, Baralle FE, Akiyama H, Hasegawa M. Phosphorylated and ubiquitinated TDP-43 pathological inclusions in ALS and FTLD-U are recapitulated in SH-SY5Y cells. FEBS Lett 2009; 583: 394–400.

Olzmann JA, Li L, Chudaev MV, Chen J, Perez FA, Palmiter RD, et al. Parkin-mediated K63-linked polyubiquitination targets misfolded DJ-1 to aggresomes via binding to HDAC6. J Cell Biol 2007; 178: 1025–38.

Pikkarainen M, Hartikainen P, Alafuzoff I. Ubiquitinated p62-positive, TDP-43-negative inclusions in cerebellum in frontotemporal lobar degeneration with TAR DNA binding protein 43. Neuropathology 2010; 30: 197–9.

Polymenidou M, Lagier-Tourenne C, Hutt KR, Huelga SC, Moran J, Liang TY, et al. Long pre-mRNA depletion and RNA missplicing contribute to neuronal vulnerability from loss of TDP-43. Nat Neurosci 2011; 14: 459–68.

Rademakers R. C9orf72 repeat expansions in patients with ALS and FTD. Lancet Neurol 2012; 11: 297–8.

Rascovsky K, Hodges JR, Knopman D, Mendez MF, Kramer JH, Neuhaus J, et al. Sensitivity of revised diagnostic criteria for the behavioural variant of frontotemporal dementia. Brain 2011; 134: 2456–77.

Reinhard E, Adhikhmin M, Gooch B, Shirley P. Color transfer between images. IEEE Comput Grap Appl 2001; 21: 34–41.

Renton AE, Majounie E, Waite A, Simón-Sánchez J, Rollinson S, Gibbs JR, et al. A hexanucleotide repeat expansion in C9ORF72 is the cause of chromosome 9p21-linked ALS-FTD. Neuron 2011; 72: 257–68.

Richter-Landsberg C, Leyk J. Inclusion body formation, macroautophagy, and the role of HDAC6 in neurodegeneration. Acta Neuropathol 2013; 126: 793–807.

Ross CA, Poirier MA. Protein aggregation and neurodegenerative disease. Nat Med 2004; 10 (Suppl): S10–7.

Ross CA, Poirier MA. Opinion: what is the role of protein aggregation in neurodegeneration? Nat Rev Mol Cell Biol 2005; 6: 891–8.

Sabatelli M, Zollino M, Conte A, D, Grande A, Marangi G, Lucchini M, et al. Primary fibroblasts cultures reveal TDP-43 abnormalities in amyotrophic lateral sclerosis patients with and without SOD1 mutations. Neurobiol Aging 2015; 36: 2005.e5–e13.

Scotter EL, Vance C, Nishimura AL, Lee YB, Chen HJ, Urwin H, et al. Differential roles of the ubiquitin proteasome system and autophagy in the clearance of soluble and aggregated TDP-43 species. J Cell Sci 2014; 127 (Pt 6): 1263–78.

Seelaar H, Schelhaas HJ, Azmani A, Kusters B, Rosso S, Majoor-Krakauer D, et al. TDP-43 pathology in familial frontotemporal dementia and motor neuron disease without Progranulin mutations. Brain 2007; 130 (Pt 5): 1375–85.

Seilhean D, Cazeneuve C, Thuries V, Russaouen O, Millecamps S, Salachas F, et al. Accumulation of TDP-43 and alpha-actin in an amyotrophic lateral sclerosis patient with the K17I ANG mutation. Acta Neuropathol 2009; 118: 561–73.

Sephton CF, Cenik B, Cenik BK, Herz J, Yu G. TDP-43 in central nervous system development and function: clues to TDP-43-associated neurodegeneration. Biol Chem 2012; 393: 589–94.

Serebryannyy LA, Cruz CM, de Lanerolle P. A role for nuclear actin in HDAC 1 and 2 regulation. Sci Rep 2016; 6: 28460.

Sha SJ, Takada LT, Rankin KP, Yokoyama JS, Rutherford NJ, Fong JC, et al. Frontotemporal dementia due to C9ORF72 mutations: clinical and imaging features. Neurology 2012; 79: 1002–11.

Shahheydari H, Ragagnin A, Walker AK, Toth RP, Vidal M, Jagaraj CJ, et al. Protein quality control and the amyotrophic lateral sclerosis/frontotemporal dementia continuum. Front Mol Neurosci 2017; 10: 119.

Shaiken TE, Opekun AR. Dissecting the cell to nucleus, perinucleus and cytosol. Sci Rep 2014; 4: 4923.

Shiarli AM, Jennings R, Shi J, Bailey K, Davidson Y, Tian J, et al. Comparison of extent of tau pathology in patients with frontotemporal dementia with Parkinsonism linked to chromosome 17 (FTDP-17), frontotemporal lobar degeneration with Pick bodies and early onset Alzheimer's disease. Neuropathol Appl Neurobiol 2006; 32: 374–87.

Sontag EM, Vonk WIM, Frydman J. Sorting out the trash: the spatial nature of eukaryotic protein quality control. Curr Opin Cell Biol 2014; 26: 139–46.

Soto C, Pritzkow S. Protein misfolding, aggregation, and conformational strains in neurodegenerative diseases. Nat Neurosci 2018; 21: 1332–40.

Swarup V, Phaneuf D, Bareil C, Robertson J, Rouleau GA, Kriz J, et al. Pathological hallmarks of amyotrophic lateral sclerosis/frontotemporal lobar degeneration in transgenic mice produced with TDP-43 genomic fragments. Brain 2011; 134: 2610–26.

Sweeney P, Park H, Baumann M, Dunlop J, Frydman J, Kopito R, et al. Protein misfolding in neurodegenerative diseases: implications and strategies. Transl Neurodegener 2017; 6: 6.

Takalo M, Salminen A, Soininen H, Hiltunen M, Haapasalo A. Protein aggregation and degradation mechanisms in neurodegenerative diseases. Am J Neurodegener Dis 2013; 2: 1–14.

Tan RH, Yang Y, Kim WS, Dobson-Stone C, Kwok JB, Kiernan MC, et al. Distinct TDP-43 inclusion morphologies in frontotemporal lobar degeneration with and without amyotrophic lateral sclerosis. Acta Neuropathol Commun 2017; 5: 76.

Taylor JP, Tanaka F, Robitschek J, Sandoval CM, Taye A, Markovic-Plese S, et al. Aggresomes protect cells by enhancing the degradation of toxic polyglutamine-containing protein. Hum Mol Genet 2003; 12: 749–57.

Troakes C, Maekawa S, Wijesekera L, Rogelj B, Siklos L, Bell C, et al. An MND/ALS phenotype associated with C9orf72 repeat expansion: abundant p62-positive, TDP-43-negative inclusions in cerebral cortex, hippocampus and cerebellum but without associated cognitive decline. Neuropathology 2012; 32: 505–14.

Turturici G, Sconzo G, Geraci F. Hsp70 and its molecular role in nervous system diseases. Biochem Res Int 2011; 2011: 618127.

Umoh ME, Dammer EB, Dai J, Duong DM, Lah JJ, Levey AI, et al. A proteomic network approach across the ALS-FTD disease spectrum resolves clinical phenotypes and genetic vulnerability in human brain. EMBO Mol Med 2018; 10: 48–62.

Umoh ME, Fournier C, Li Y, Polak M, Shaw L, Landers JE, et al. Comparative analysis of C9orf72 and sporadic disease in an ALS clinic population. Neurology 2016; 87: 1024–30.

van Eersel J, Ke YD, Gladbach A, Bi M, Gotz J, Kril JJ, et al. Cytoplasmic accumulation and aggregation of TDP-43 upon proteasome inhibition in cultured neurons. PLoS One 2011; 6: e22850.

Vatsavayai SC, Yoon SJ, Gardner RC, Gendron TF, Vargas JN, Trujillo A, et al. Timing and significance of pathological features in C9orf72 expansion-associated frontotemporal dementia. Brain 2016; 139 (Pt 12): 3202–16.

Walker AK, Soo KY, Sundaramoorthy V, Parakh S, Ma Y, Farg MA, et al. ALS-associated TDP-43 induces endoplasmic reticulum stress, which drives cytoplasmic TDP-43 accumulation and stress granule formation. PLoS One 2013; 8: e81170.

Webber E, Li L, Chin LS. Hypertonia-associated protein Trak1 is a novel regulator of endosome-to-lysosome trafficking. J Mol Biol 2008; 382: 638–51.

Wils H, Kleinberger G, Janssens J, Pereson S, Joris G, Cuijt I, et al. TDP-43 transgenic mice develop spastic paralysis and neuronal inclusions characteristic of ALS and frontotemporal lobar degeneration. Proc Natl Acad Sci USA 2010; 107: 3858–63.

Wojciechowska M, Krzyzosiak WJ. Cellular toxicity of expanded RNA repeats: focus on RNA foci. Hum Mol Genet 2011; 20: 3811–21.

Yang C, Tan W, Whittle C, Qiu L, Cao L, Akbarian S, et al. The C-terminal TDP-43 fragments have a high aggregation propensity and harm neurons by a dominant-negative mechanism. PLoS One 2010; 5: e15878.

Zaarur N, Meriin AB, Gabai VL, Sherman MY. Triggering aggresome formation. Dissecting aggresome-targeting and aggregation signals in synphilin 1. J Biol Chem 2008; 283: 27575–84.

Zhang K, Donnelly CJ, Haeusler AR, Grima JC, Machamer JB, Steinwald P, et al. The C9orf72 repeat expansion disrupts nucleocytoplasmic transport. Nature 2015; 525: 56–61.